NOAA TECHNICAL MEMORANDUM
NWS WR-244

WSR-88D VAD WIND PROFILE DATA INFLUENCED BY BIRD MIGRATION OVER THE SOUTHWEST UNITED STATES

Jesus Haro
National Weather Service Forecast Office
Phoenix, Arizona

Sydney Gauthreaux
Clemson University

January 1997

This publication has been reviewed and is approved for publication by Scientific Services Division, Western Region

Delain A. Edman, Chief
Scientific Services Division
Salt Lake City, Utah

TABLE OF CONTENTS

TABLE OF FIGURES

WSR-88D VAD WIND PROFILE DATA INFLUENCED BY BIRD MIGRATION OVER THE SOUTHWEST UNITED STATES

Jesus A. Haro
National Weather Service Forecast Office
Phoenix, Arizona

Sydney A. Gauthreaux, Jr.
Department of Biological Sciences
Clemson University

Abstract

Since the acceptance of the WSR-88D in Phoenix, Arizona (KIWA), NWSFO Phoenix forecasters have been continually cognizant of an odd pattern of strong low-level winds apparent in the KIWA WSR-88D's Velocity Azimuth Display Wind Profile (VWP) during the hot late spring and summer months. Frequent, and surprisingly strong, derived winds from the southeast to south at speeds up to 40 kts are commonly represented in these profiles during the nighttime and early morning hours. The winds encompass a vertical area stretching from near the surface to around 15,000 ft MSL, begin shortly after sunset, and last several hours. Confusion among the forecasters stemmed from the fact that the southwest U.S. is dominated by light wind flow regimes during the warm season. The wind patterns in the VWP are rarely representative of true environmental conditions in the lower atmosphere or supported synoptically. It has been argued that this is clearly an example of VWP contamination, most likely caused by migrating birds. However, these patterns are not exclusive to the KIWA WSR-88D and can be found at other RDA sites across the southwestern U.S. Operationally, these discrepancies are significant as data from the WSR-88D VWP are often used for briefing and research purposes. In this report, three distinct examples are used to relate migrating bird patterns over the southwest U.S. to contaminated WSR-88D output via the VWP.

I. INTRODUCTION

The WSR-88D's VAD Wind Profile (VWP) has proven to be a valuable tool to operational and research meteorologists. When convective storms develop, forecasters use the VWP to assess the potential for multicell and supercell storms, and to predict likely storm movement and propagation.

Additionally, aviation forecasters have found that the VWP is useful for detecting low-level wind shear (LLWS) and for briefing purposes. However, the radar has also proven to be an excellent detector of non-meteorological phenomena, especially migrating birds. For this reason, it is of the utmost importance to verify VAD-derived winds.

The operational implications involved with using or disseminating contaminated VWP data are many. The use of contaminated data for forecast purposes can have substantial negative effects. Similarly, disseminating output from the VWP either verbally or as part of a briefing can be hazardous if it is unrepresentative of the environmental conditions present around the radar site. Yet all too often, the VAD-derived output is assumed to be representative of the environment surrounding the radar.

Since its acceptance in March 1993, the KIWA radar site has continually detected a strong south to southeast wind flow in the lower levels of the atmosphere in its immediate vicinity. These winds are strongest during the hot late spring and summer months and can reach speeds as high as 40 knots. Typically these winds begin shortly after sunset and last for several hours at night, usually abating a couple of hours before sunrise.

Many of the characteristics associated with bird migration over the southwest U.S. (liftoff times, flight speeds, direction of movement) are consistent with anomalous products produced by the KIWA WSR-88D. This Technical Memorandum relates bird migration patterns over the southwest U.S. to WSR-88D output by using examples in which environmental meteorological conditions did not support the VWP output.

II. BIRD MIGRATION CHARACTERISTICS AND THE WSR-88D

Historically, weather surveillance radars have been used to study the migration of birds (Gauthreaux 1970). These systems readily detect birds in the atmosphere, and much of what we know about en route bird migration has been gathered using surveillance and tracking radars.

Most bird migration occurs at night. Typically, birds depart en route stopover areas 30-45 minutes after sunset (Gauthreaux 1991). During the evening, songbirds tend to fly alone while waterfowl and shorebirds fly in flocks (Gauthreaux 1991). Although most migrating songbirds at night typically fly at altitudes below 2100 ft (Gauthreaux 1991), waterfowl migration may occur up to 21,000 ft MSL (Bellrose 1976). Flight speeds of migrating birds vary depending on the size and type of bird such that the speed roughly doubles when the mass of the bird increases 100 times up to the limit of 15-20 kg when flying is not possible (Berthold 1996:168). During migration, average flight speeds range from about 15 to 35 kts for songbirds and from 25 to 45 kts for waterfowl and shorebirds (Alerstam 1990, Evans and Davidson 1990).

Only one radar study has examined the migration of birds over the southwestern United States, and although the emphasis of the study was on waterfowl migration

(Beason 1978, 1980), some information on songbird migration was gathered (Beason 1976: 13-14). He noted that the highest rates of migration almost invariably occurred at night between 2200 and 2400 local time at altitudes between 1,500 and 6,000 ft AGL, and that migration to the north occurred under all wind conditions but was most common with tailwinds.

Although migrating birds have been shown to contaminate wind profiler data (Wilczak et al. 1995), case histories of birds biasing wind data on the VAD and VWP products of the WSR-88D are few (Larkin 1991, Jungbuth 1993, Gauthreaux in prep.). Since 1992, one of the authors (SAG) has studied bird migration detected on the WSR-88D and discovered numerous cases when the VAD and VWP products of the WSR-88D were contaminated by bird migration.

In most instances, migrating birds fly with tailwinds and bias wind speeds upward by 15 to 20 kts, but in several cases, the direction of the winds on the VWP were severely biased (e.g., 90-180° difference) when migrating birds were flying north and the winds were light and from the east and west, or from the north.

Such cases clearly indicate that migrating birds have been included as reflectors in the VAD algorithm. Most migrating songbirds have air speeds between 15 and 30 kts and most adjust their air speeds downward as a function of the speed of the tailwind. Concentrations of insects can also be detected by the WSR-88D and similar surveillance radars (Russell and Wilson 1996), but insect air speeds rarely exceed 20 kts and are typically in the 8-10 kt range (e.g., Riley et al. 1996).

III. METHODOLOGY

Three cases are shown which verify that the winds produced on several VAD Wind Profiles are not representative of environmental conditions at the radar sites. Eta model PCGRIDDS output for 0000 UTC 12 May 1996, 0000 UTC 18 May 1996 and 0000 UTC 02 June 1996 was used.

Analyses at the 850 mb, 700 mb, and 500 mb levels were reproduced. Overlaid were the geopotential heights (meters), relative humidity (tens of %) and wind (kts) to represent the atmospheric conditions at the time of initial analysis. In one of the cases, these analyses and two upper air soundings (Tucson and Flagstaff) were compared to VAD Wind Profile output to show that the output was not supported synoptically.

VAD Wind Profiles for six RDA sites across the southwest U.S. (Phoenix, Tucson, Flagstaff, Las Vegas, San Diego, and Albuquerque) were used in Case 1. Only data from central Arizona and the KIWA (Phoenix) radar site were used for Cases 2 and 3. Additionally, for Case 2, KIWA VAD Wind Profile data are compared to pilot balloon (Pibal) flight data. These data were collected approximately one mile west of the radar site.

IV. CASE 1: 11-12 MAY 1996

Eta model initial analyses for 0000 UTC 12 May 1996 generated from PCGRIDDS were chosen for this case because of the model's excellent handling of the relative humidity and wind conditions over the southwest U.S. for these dates. Satellite imagery and surface observations (not shown) confirmed that clear skies covered much of the southwest U.S.

At the 850 mb level (Fig. 1), a weak cyclonic circulation is evident off the central California coast with a much stronger system off the British Columbia coast. Light winds of 10 knots or less are evident across most of the southwestern states. The highest relative humidity values are off the Pacific Northwest coast, associated with the British Columbia system. The dry low-level conditions that were present across the western states are well represented in this figure.

A similar pattern is evident at 700 mb (Fig. 2). The main difference is that the higher relative humidity values are concentrated inland along the U.S.-Canada border. Relatively light winds and dry conditions are clearly evident at this level as well.

A ridge of high pressure is very evident at the 500 mb level over the southwest U.S. (Fig. 3) with a weak trough off the central California coast and a stronger trough in the Gulf of Alaska. At this time, the closest mid- and high-level cloudiness to any of the RDA sites in question was moving into southern Oregon. This is captured well by the Eta model PCGRIDDS relative humidity analysis at this level. Pronounced southwest winds are evident flowing into central California and Nevada with the main jet stream moving into the Pacific Northwest.

VAD Wind Profiles from RDA sites across the southwest U.S. (Figs. 4-9) reveal relatively strong southeast to south winds to be prevalent across much of the southwest U.S. Specifically, the VWP output from the KIWA (Phoenix), KEMX (Tucson), KFSX (Flagstaff), and KESX (Las Vegas) radars (Figs. 4-7) is quite similar.

These four sites exhibit southeast winds at speeds ranging from 15 to 30 kts. The vertical extents of these winds are very similar, with the winds extending to around 17,000 ft MSL on all of the profiles. Additionally, the profiles took this configuration between 0300 UTC and 0400 UTC 12 May 1996 (not shown).

The KIWA base reflectivity product at 1.5° for 0657 UTC 12 May 1996 (Fig. 10a) shows a large area of relatively high reflectivities surrounding the RDA site. The 1.5° base velocity product for the same time period (Fig. 10b) shows a pronounced southeast flow and corresponds well to the VWP.

The KEMX (Tucson) VWP for early that morning (Fig. 11a) compares poorly to the Tucson upper-air sounding for 1200 UTC 12 May 1996 (Fig. 11b). A pronounced southeast flow is present on the VWP at speeds primarily around 20 kts. The sounding has light north winds up to about 7,000 ft MSL, before shifting to a southerly and then southwesterly

direction between 10,000 and 15,000 ft MSL.

Similar discrepancies can be found when comparing the KFSX (Flagstaff) VWP (Fig. 12a) with their morning sounding (Fig. 12b). The VWP has strong south to southeast winds of 20 to 30 kts in south-southeasterly (direction from 8,000 ft to about 13,000 ft MSL). The sounding, however, has light north winds near the surface with south winds of 10 to 15 kts between 10,000 and 15,000 ft MSL.

The other RDA sites exhibit similar VAD Wind Profiles. With clear skies around the Region, it seems uncertain as to why these strong winds are apparent on all of the profiles, given an apparent lack of low and mid level meteorological scatterers.

V. CASE 2: 17-18 MAY 1996

For this case, a comparison of the KIWA VWP to atmospheric conditions over central Arizona is made. As with the first case, the Eta model was chosen because of its good initial analysis of the prevalent atmospheric conditions. Data from 0000 UTC 18 May 1996 reproduced from PCGRIDDS are used for this case.

An examination of 850 mb, 700 mb, and 500 mb data (Figs. 13-15), reveals that a fast-moving low-pressure trough had just skirted northern Arizona the previous day and was well northeast of the state, and that another trough was impacting northern California and the Sierra Nevada.

At the 850 mb level (Fig. 13), weak shortwave ridging is evident behind the low-pressure trough. Weak southwest to west flow is evident across central Arizona at speeds of less than 10 kts. Dry low-level conditions behind the trough are well represented.

A pronounced west flow is also evident at 700 mb (Fig. 14) behind the fast-moving shortwave. Again, dry conditions are highly prevalent across central Arizona.

At the 500 mb level (Fig. 15), flat ridging is evident across central Arizona with the most substantial relative humidity values and strongest winds well to the north of Arizona. Surface observations (not shown) revealed that only thin cirriform cloudiness was present across central Arizona.

A Pibal observation was taken at approximately 2235 MST 17 May 1996 in order to complement the upper air plot data. This was necessary since no routine soundings are taken at Phoenix. The balloon was released approximately one mile west of the KIWA radar site. The results of this flight again (Fig. 16) confirm the presence of a southwest to west flow from the surface up to about 10,000 ft AGL.

These data suggest that the KIWA radar VWP winds would have a southwest to west component. Rather, the VWP corresponding to the time of the Pibal flight (Fig. 17), shows the winds to again have a southeast to south orientation, especially between 5,000 and 10,000 ft MSL.

There was a pronounced lack of meteorological scatterers present across central Arizona, except for the cirriform clouds. Again, this is not consistent with the KIWA VWP output.

VI. CASE 3: 01-02 JUNE 1996

For this case, data from the KIWA WSR-88D were compared with Eta model initial conditions. Eta model data from the 0000 UTC 02 June 1996 model run reproduced from PCGRIDDS were used. Skies were predominantly clear (not shown) with no discernable meteorological scatterers. A light wind-flow regime was in place with high pressure over the southwest U.S. (Figs. 18-20).

At 850 mb (Fig. 18), winds over Arizona were variable at under 10 kts, but generally from the west over Phoenix. Relative humidity values were very low.

Similarly, the wind pattern at 700 mb over Arizona (Fig. 19) was also weakly defined. A deformation zone was present over central Arizona with light and variable winds. Again, relative humidity values were very low.

At the 500 mb level (Fig. 20), a strong 5940 meter ridge is present over the state. Accordingly, winds are light and variable (under 10 kts) with low relative humidity values over the state.

The KIWA VAD Wind Profile for 0330 UTC 02 June 1996 (Fig. 21) depicted light and variable winds until around 0330 UTC, when east winds at around 15 kts begin to appear at around 10,000 ft MSL.

An inspection of the VAD Wind Profile for 0508 UTC (Fig. 22) that same evening reveals that the layer of easterly winds expanded vertically and reached a depth of 8,000 ft. MSL. Easterly winds increased to 30 kts, and were consistent through a layer from around 8,000 to 16,000 ft MSL.

A KIWA base reflectivity product valid at 0824 UTC 02 June 1996 (Fig. 23a) at the 2.5° elevation slice, shows reflectivity maxima to the northeast and southwest of the RDA site. The height of the beam center at the locations of highest reflectivities is between 10,000 ft and 11,000 ft MSL. The base velocity product showed a stiff east-southeast wind (Fig. 23b) at speeds of 20 to 40 kts.

The VAD Wind Profile pattern begins to dissolve later that night (Fig. 24). The profile shows a decreasing southeast wind after about 1100 UTC.

Clearly, the winds apparent on the VWP and base velocity products are not supported synoptically. It is possible that output from these VWPs could be misinterpreted as representing a mesoscale phenomena or as suggesting that model initial conditions are poor.

VII. DISCUSSION

The WSR-88D products shown in the aforementioned cases display characteristics representative of bird migration. During the late spring and early summer, considerable bird migration, including late-migrating waterfowl, shorebirds, and songbirds, is

underway in the southwest U.S. (see seasonal occurrence charts in Davis and Russell 1990).

The base reflectivity image from Case 1 valid at 0657 UTC 12 May 1996 (Fig. 10a) depicts a pattern typically observed during nocturnal bird migration. This "explosion" of reflectivity values shortly after sunset can be expected during times of migration from en route stopover areas. The corresponding base velocity product (Fig. 10b), showing the migration occurring to the northwest, is representative of the type of migration that occurs over the southwest U.S. during the late spring and early summer.

The northwest direction of flight is apparent on all Case 1 VAD Wind Profiles (Figs. 4-7). The speeds represented on the VWPs are also consistent with songbird migration air speeds.

The Case 2 VWP and base velocity products are similarly biased by migrating birds. Initial analyses and Pibal measurements verified that environmental westerly flow was present (Figs. 13-16). However, the VWP depicted southeast-south winds. The migrating birds were severely biasing the VWP wind directions. Differences of around 70-90° are evident between the direction of flight of the birds and the environmental flow from near the surface up to about 10,000 ft. AGL. Additionally, the migrating birds were biasing the wind speeds represented on the VWP by about 10-20 kts.

Several classic bird migration signatures are evident in the WSR-88D imagery used in Case 3. It has been established (Gauthreaux 1991) that bird migration typically ensues 30-45 minutes after sunset. The initial VWP for this case (Fig. 21) begins to display easterly winds at 0330 UTC 02 June 1996. Sunset on this date occurred at 0233 UTC. Thus, the time of the change in the VWP pattern is consistent with the observed liftoff time used by migrating birds over the southwest U.S. Inspection of the VWP shows the pattern becoming more pronounced as the evening progresses (Fig. 22).

The flight direction is consistent with what can be expected from migrating birds over the southwest U.S. during the late spring and early summer (Beason 1976: 13-14). The highest base reflectivity values are to the northeast and southwest of the radar (Fig. 23a). This is logical considering that during a northwest migration (Fig. 23b), the highest reflectivities would be at locations perpendicular to the radar beam, as these birds would return a stronger signal to the radar than the other migrating birds.

Bird migration over the southwest U.S. is a nocturnal activity. As can be seen on the last VWP for Case 3 (Fig. 24), the migratory pattern, and east wind, becomes more and more diffuse toward sunrise. At this time of day, the birds arrive at en route stopover areas to feed until they depart the next evening.

VIII. CONCLUSIONS

The anomalous WSR-88D wind fields used in this paper from the KIWA WSR-

88D and several other radars across the southwestern U.S. display characteristics consistent with those displayed by radars that have tracked migrating birds. The displays in this paper were all collected during a time of year during which bird migration over the southwest U.S. toward the north and northwest is quite pronounced (Davis and Russell 1990). Additionally, it has been shown that in none of the cases were the winds on the VWPs supported synoptically. Therefore, it is reasonable to conclude that the patterns on the VWPs used in this paper were caused by migrating birds.

These cases highlight the need to verify the VWP winds prior to use in either operational or research endeavors. Had forecasters on duty at The Phoenix forecast office used these WSR-88D data as part of a briefing, they would have been using information not representative of the meteorological environment. Similarly, researchers would have had anomalous data to work with and could have arrived at incorrect conclusions based on these data alone.

It is of the utmost importance that users of the WSR-88D verify these wind fields prior to use as part of any operational or educational endeavors. It is hoped that in the future either software or hardware changes are made to the WSR-88D so that anomalies caused by migrating birds can be identified and removed.

Acknowledgments: Thanks to Bill Estle and Bob Wilt (Lead Forecasters, NWSFO Phoenix) for their support and insight, and to Doug Green (Science and Operations Officer, NWSFO Phoenix) for his helpful review of this paper.

Very special thanks to Bob Berkovitz (Fire Weather Forecaster, NWSFO Phoenix) for executing the Pibal flight used in this study and to Tony Haffer (AM/MIC, NWSFO Phoenix) for supporting this paper.

IX. REFERENCES

Alerstam, T. 1990. Bird migration. Cambridge University Press, Cambridge, New York. 420 pp.

Beason, R. C. 1976. Water bird migration in the southwestern United States: The influence of weather and topography. Ph.D. Dissertation, Department of Zoology, Clemson University, Clemson, SC.

Beason, R. C. 1978. The influence of weather and topography on water bird migration in the southwestern United States. *Oecologia (Berl.),* **32**, 153- 169.

Beason, R. C. 1980. Orientation of waterfowl migration in the southwestern United States. *J. Wildlife Management*, **44,** 447-455.

Bellrose, F. C. 1976. Ducks, geese, and swans of North America. Stackpole, Harrisburg, Pa. 543 pp.

Berthold, P. 1996. Control of Bird Mi-ration. Chapman & Hall, London. 355 pp.

Davis, W. A. and S. M. Russell. 1990. Birds in southeastern Arizona. Tucson Audubon Society, Tucson. 154 pp.

Evans, P R. and N. C. Davidson. 1990. Migration strategies and tactics of waders breeding in arctic and north temperate latitudes. pp. 594-603. In: Bird migration: Physiology and Ecophysiology (ed. E. Gwinner). Springer, Berlin. 435 pp.

Gauthreaux, S. A., Jr. 1970. Weather radar quantification of bird migration. *BioScience,* **20**, 17-20.

Gauthreaux, S. A., Jr. 1972. Behavioral responses to migrating birds to daylight and darkness: a radar and direct visual study. *The Wilson Bulletin,* **84,** 136-148.

Jungbluth, K. 1993. Effects of migrating birds on wind speeds determined by the WSR-88D and wind profiler networks. NSSFC Operational Notes, November 1993: 1-3.

Larkin, R. P. 1991. Sensitivity of NEXRAD algorithms to echoes from birds and insects. Preprints: *Twenty-fifth International Conference on Radar Meteorology,* Paris, American Meteor. Soc., 203-205.

Operations Training Branch. 1995. WSR-88D Operations Training Student Guide. Operational Support Facility, Norman, OK.

Riley, J. R., A. D. Smith, D. R. Reynolds, A. S. Edwards, J. L. Osborne, I. H. Williams, N. L. Carreck, and G. M. Poppy. 1996. Tracking bees with harmonic radar. *Nature,* **379**, 29-30.

Russell, R. W. And J. W. Wilson. 1996. Aerial plankton detected by radar. *Nature,* **381**, 200-201.

Wilczak, J.M., R.G. Strauch, F.M. Ralph, B.L. Weber, D.A. Merritt, J.R. Jordan, D.E. Wolfe, L.K. Lewis, D.B. Wuertz, J.E. Gayrno, S.A. McLaughlin, R.R. Rogers, A.C. Riddle, and T.S. Dye. 1995. Contamination of wind profiler data by migrating birds: Characteristics of corrupted data and potential solutions. *J. Atmospheric and Oceanic Technology,* **12**, 449-467.

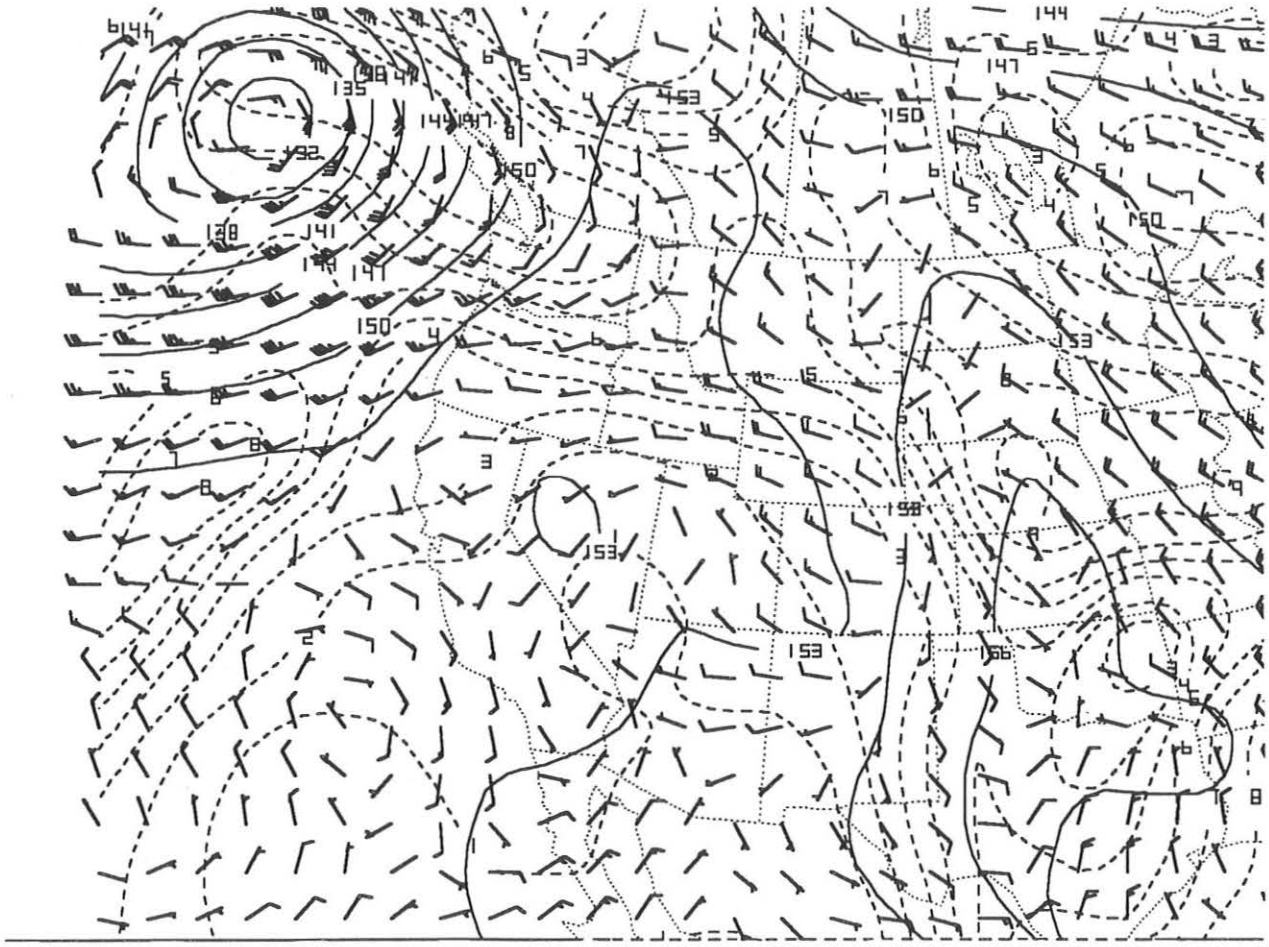

Fig. 1 ETA model PCGRIDDS initial analysis of geopotential height (dam), relative humidity (tens of %), and wind (kts) at the 850 mb level for 0000 UTC 12 May 1996

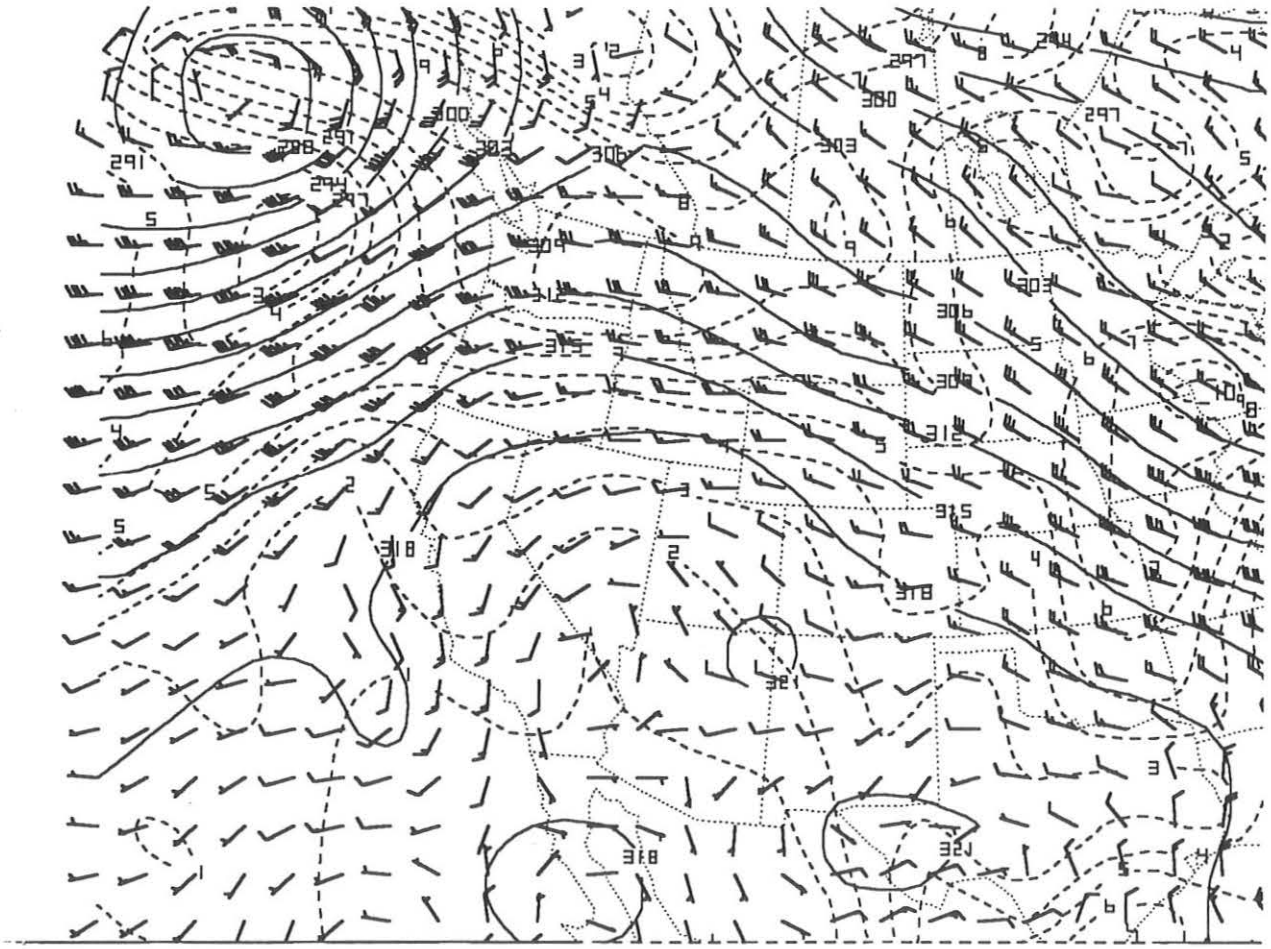

Fig. 2 ETA model PCGRIDDS initial analysis of geopotential height (dam), relative humidity (tens of %), and wind (kts) at the 700 mb level for 0000 UTC 12 May 1996

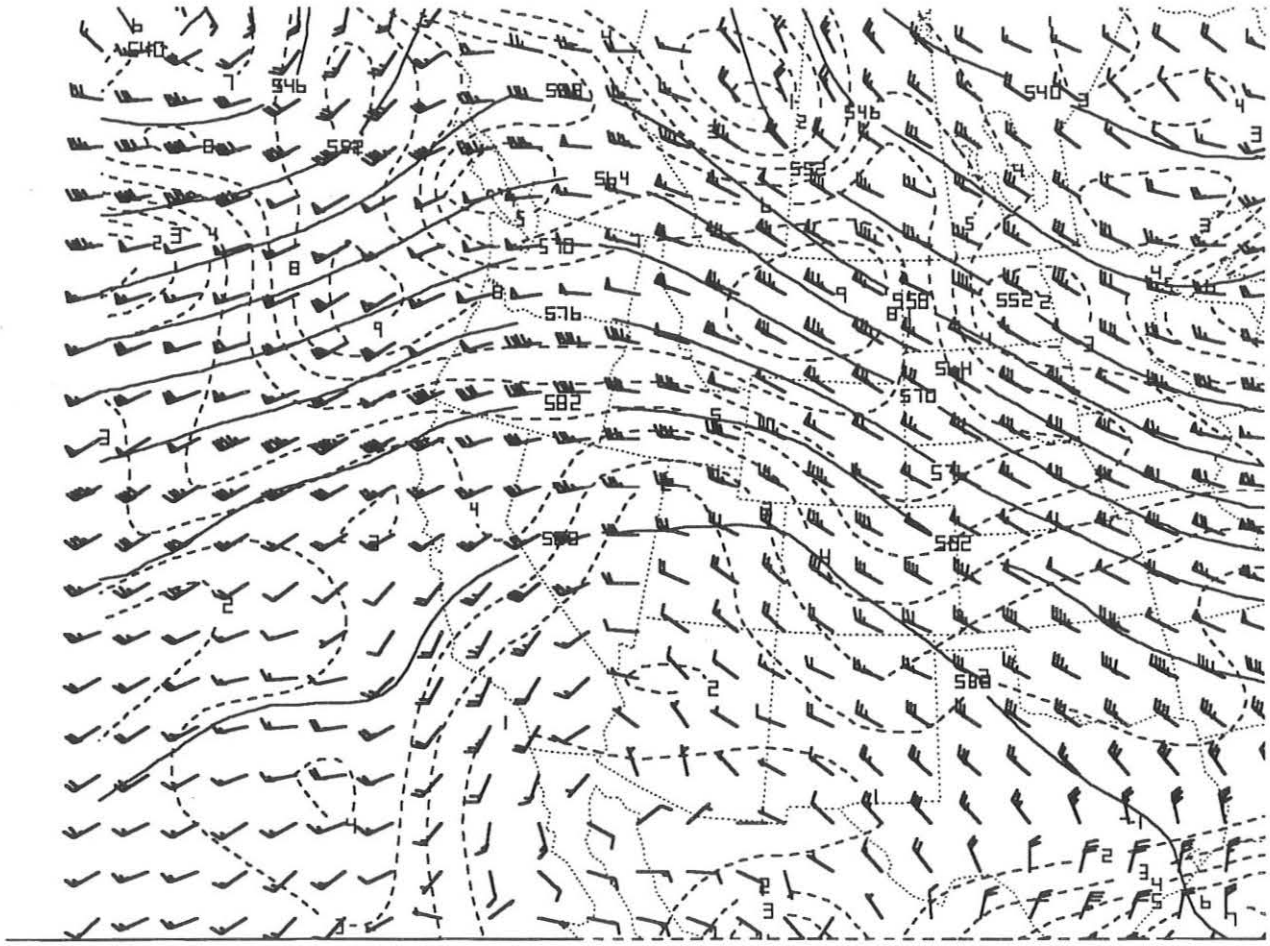

Fig. 3 ETA model PCGRIDDS initial analysis of geopotential height (dam), relative humidity (tens of %), and wind (kts) at the 500 mb level for 0000 UTC 12 May 1996

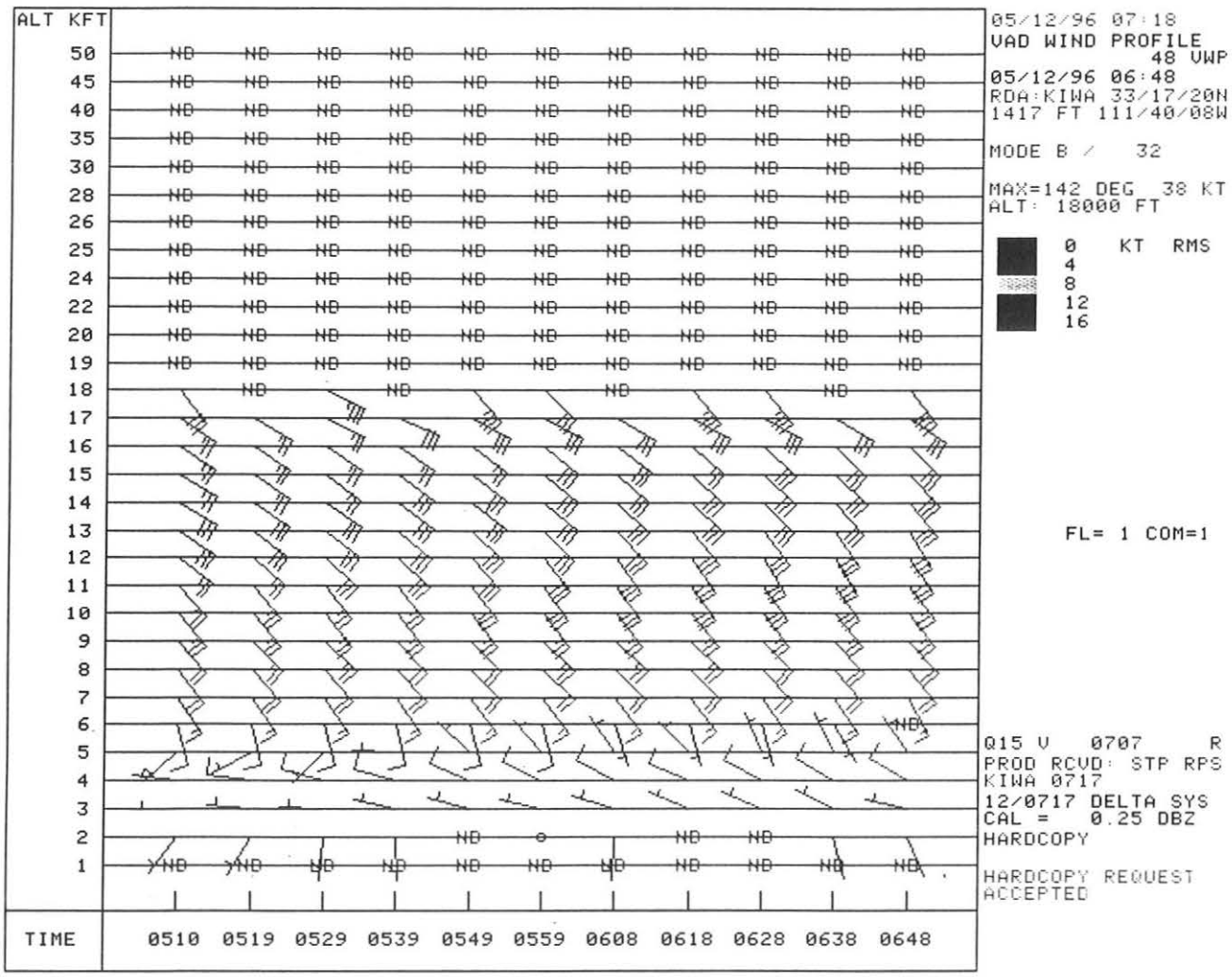

Fig. 4 KIWA (Phoenix) VAD Wind Profile for 0648 UTC 12 May 1996

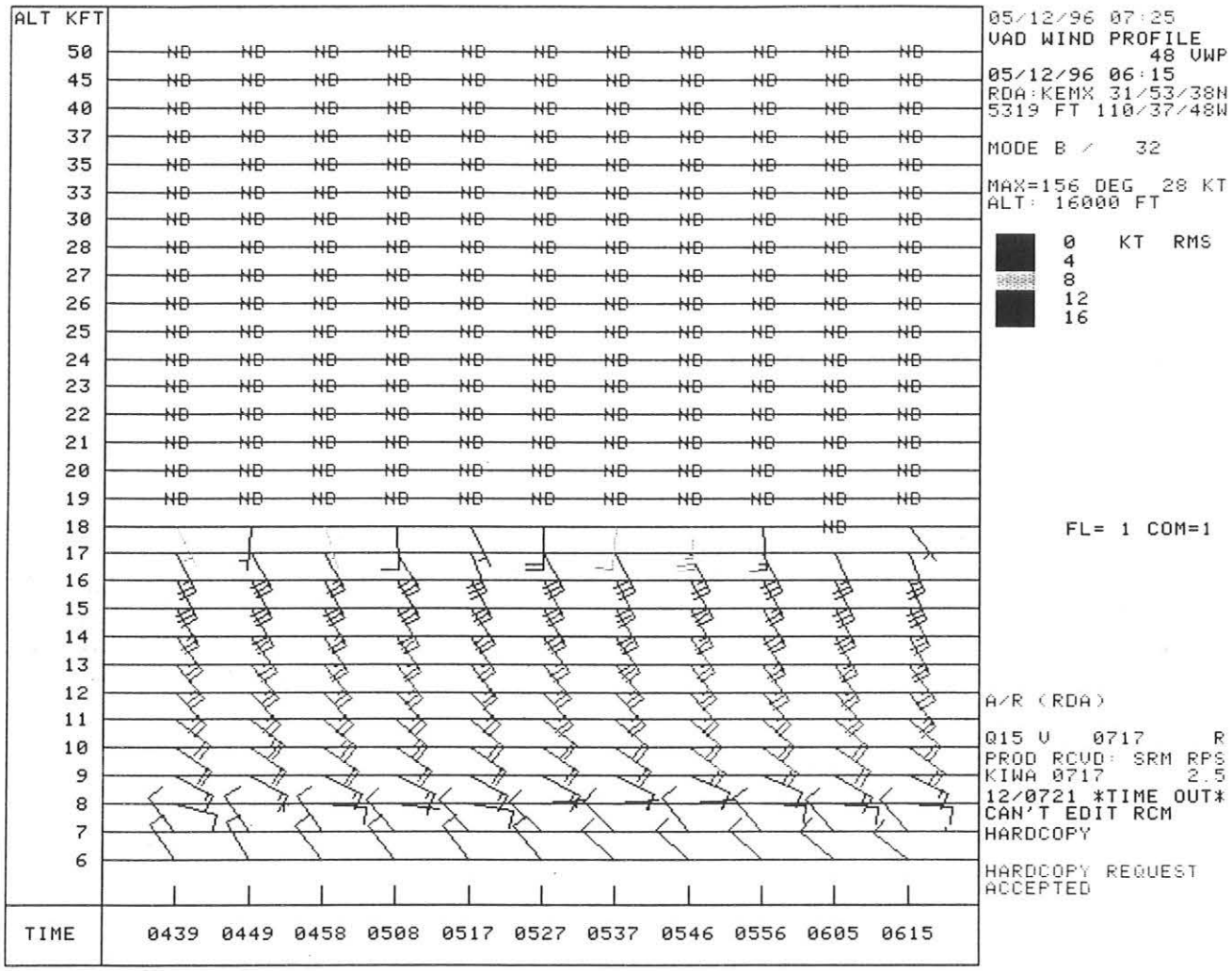

Fig. 5 KEMX (Tucson) VAD Wind Profile for 0615 UTC 12 May 1996

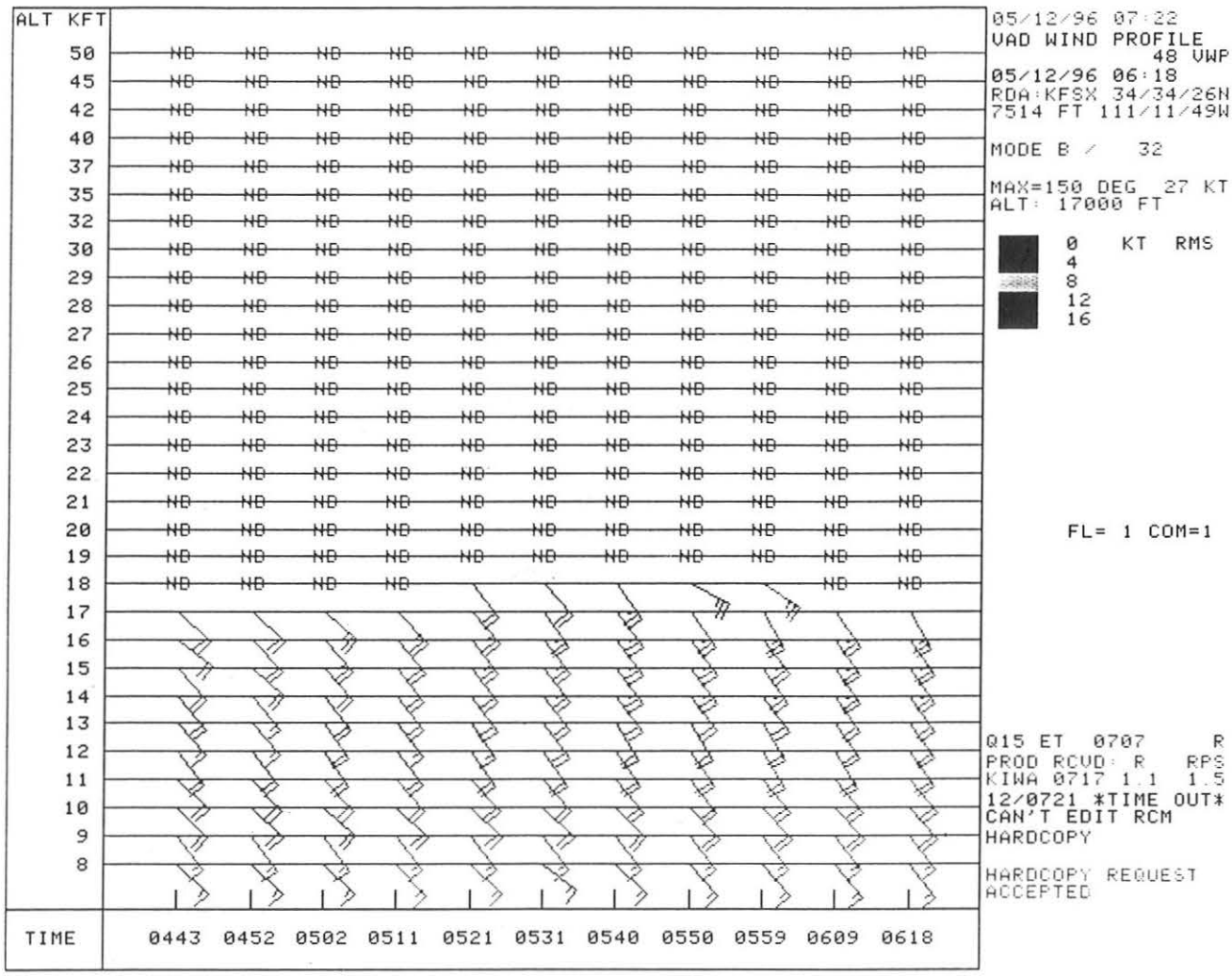

Fig. 6 KFSX (Flagstaff) VAD Wind Profile for 0618 UTC 12 May 1996

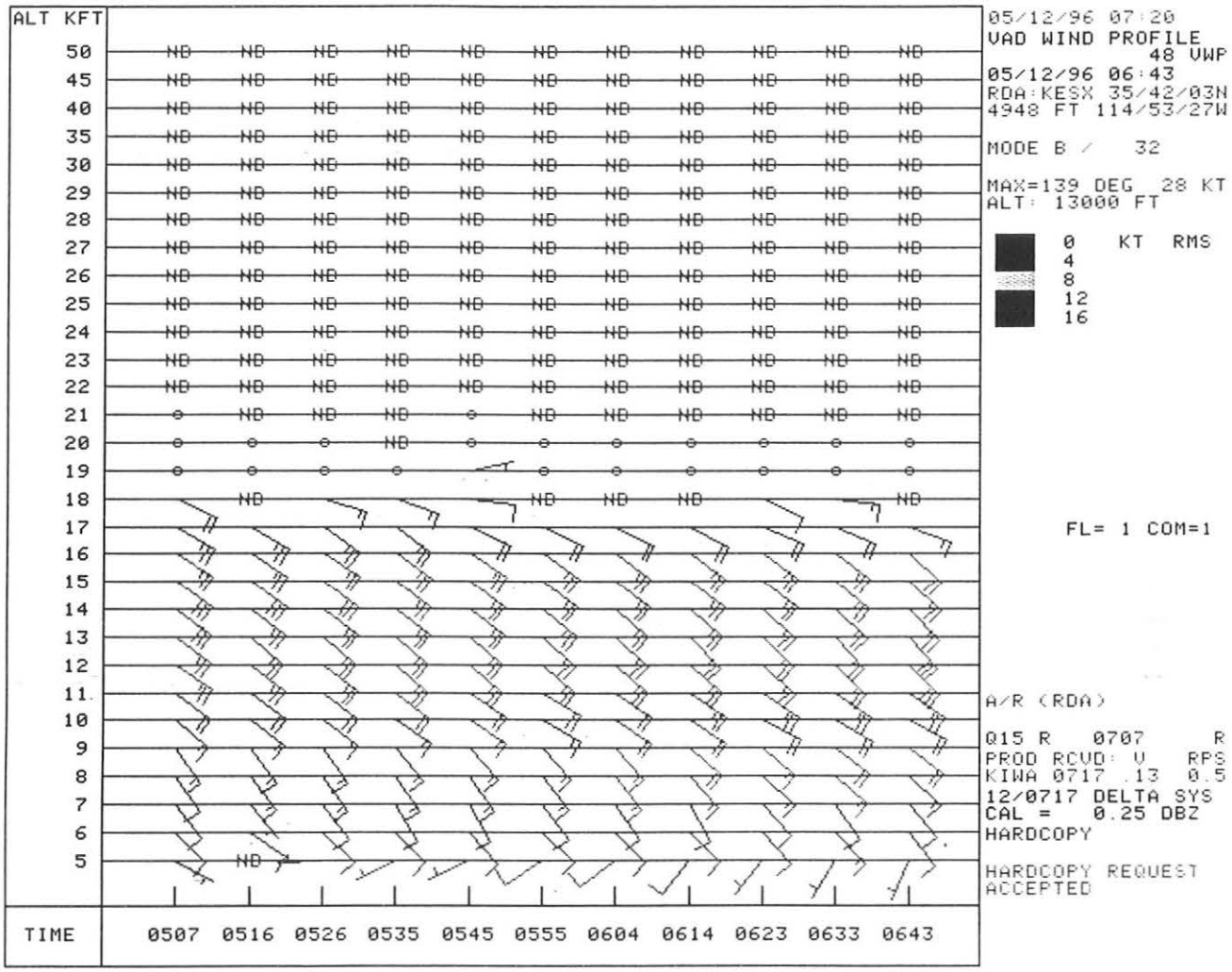

Fig. 7 KESX (Las Vegas) VAD Wind Profile for 0643 UTC 12 May 1996

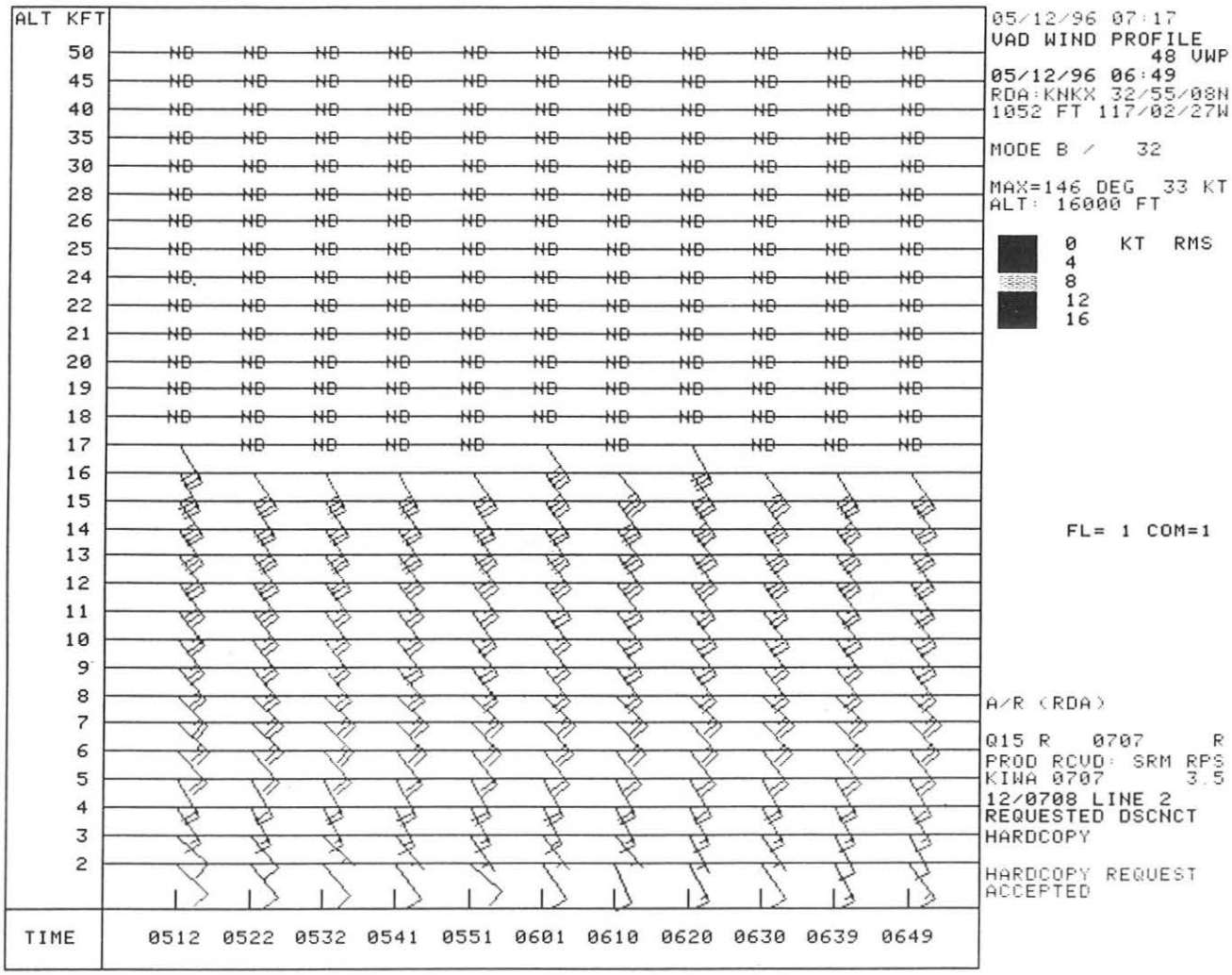

Fig. 8 KNKX (San Diego) VAD Wind Profile for 0649 UTC 12 May 1996

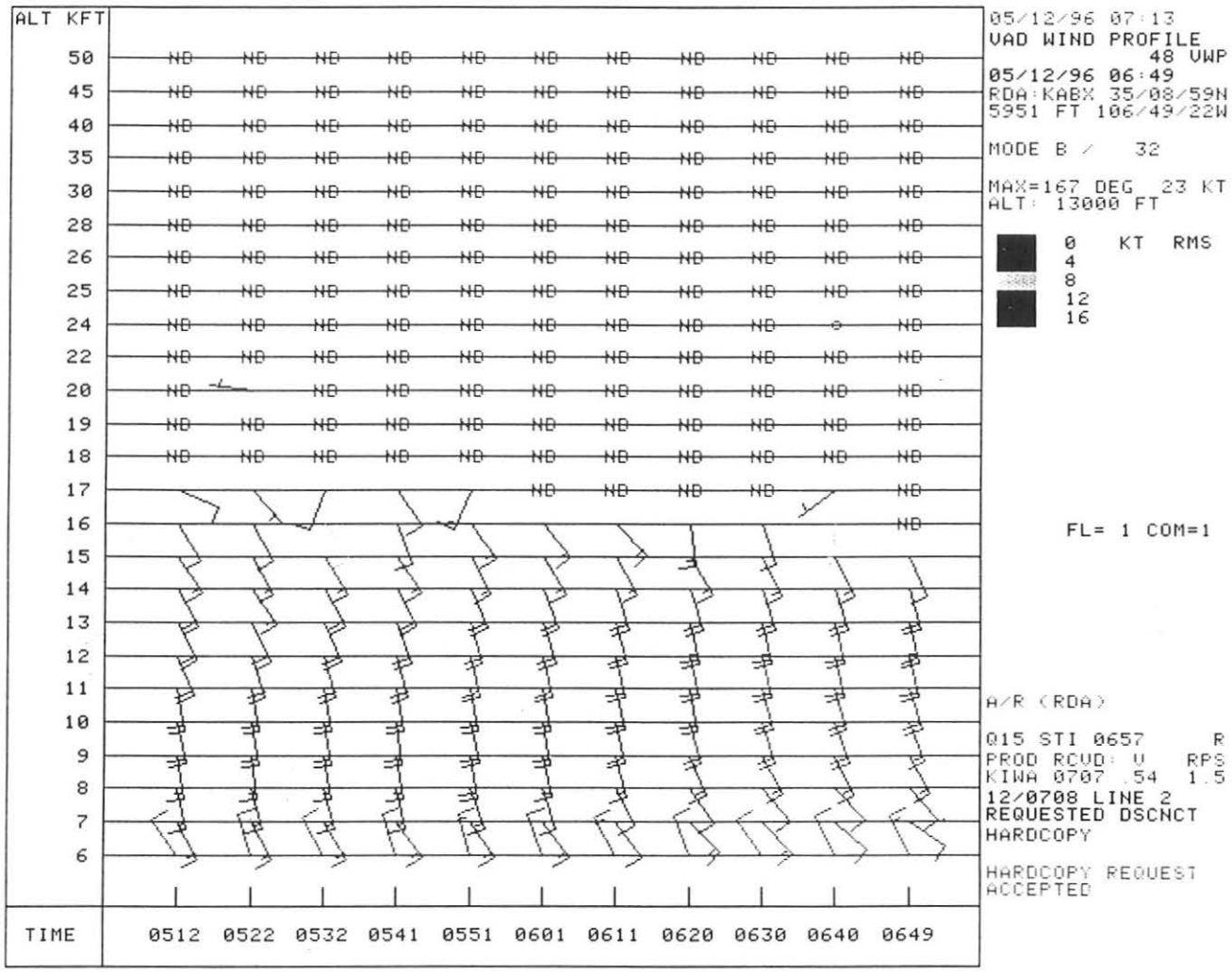

Fig. 9 KABX (Albuquerque) VAD Wind Profile for 0649 UTC 12 May 1996

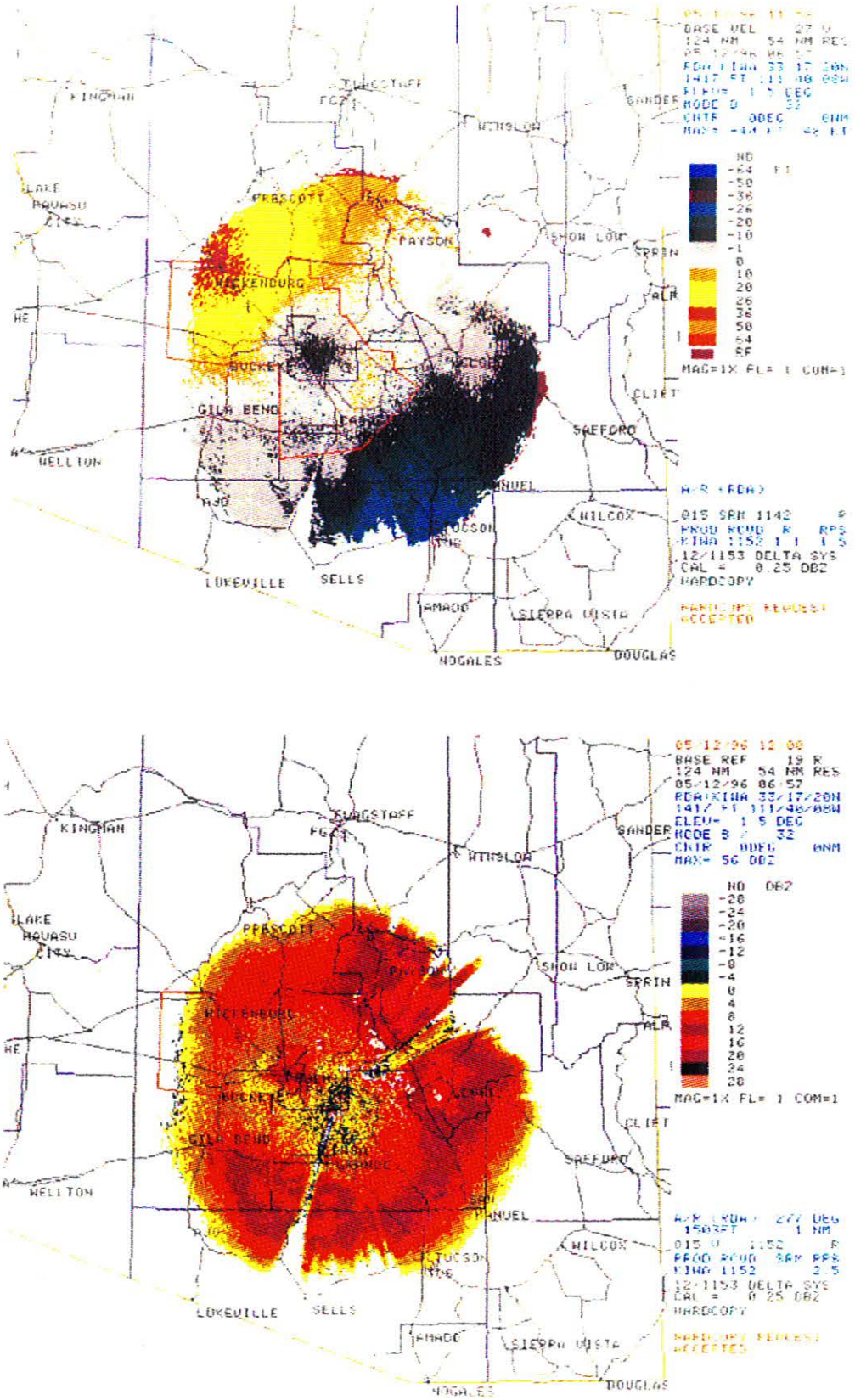

Fig. 10 (a) KIWA 1.5° Base Reflectivity and (b) Velocity products valid at 0657 UTC 12 May 1996

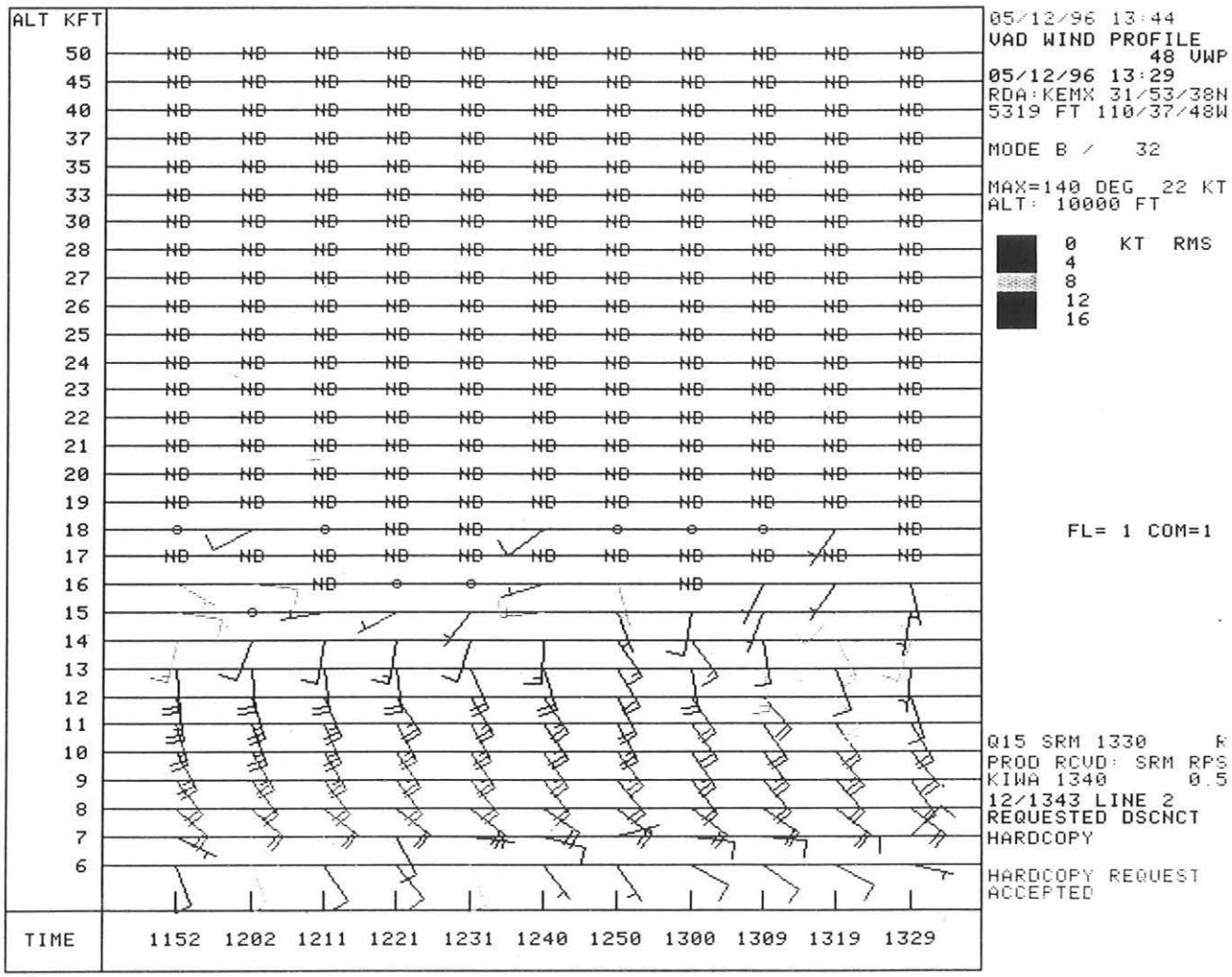

Fig. 11a KEMX (Tucson) VAD Wind Profile for 1329 UTC 12 May 1996

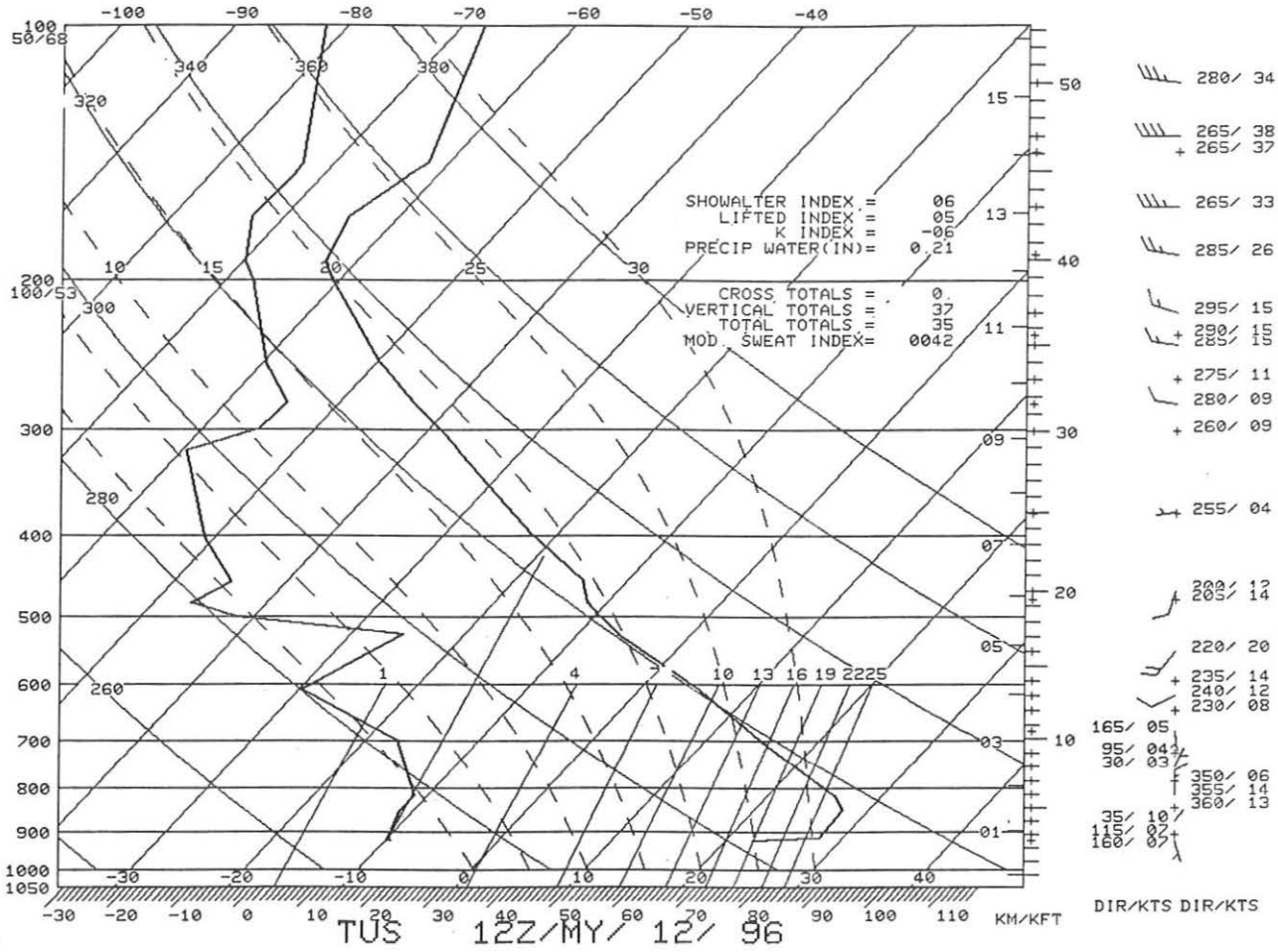

Fig. 11b TUS (Tucson) sounding for 1200 UTC 12 May 1996

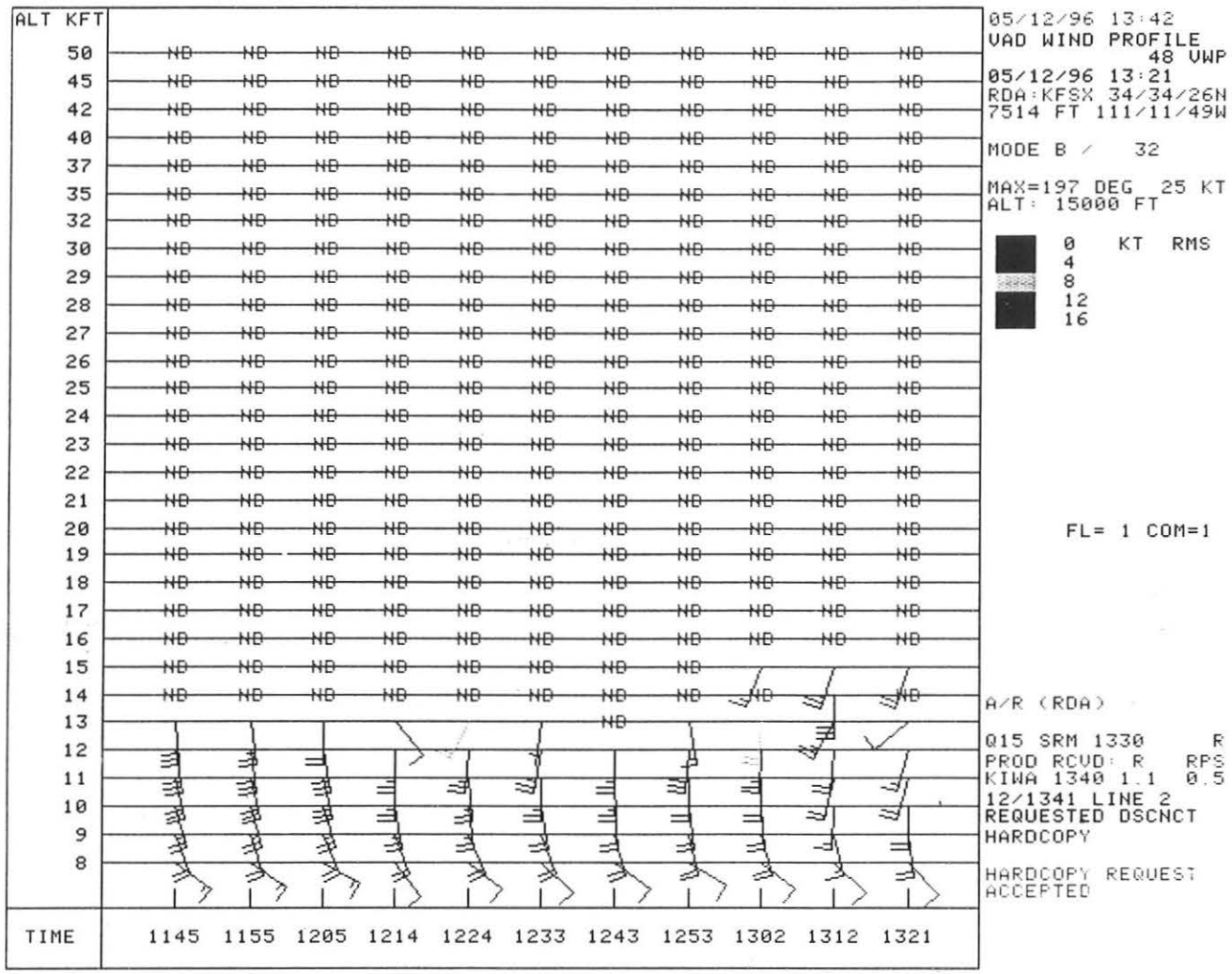

Fig. 12a KFSX (Flagstaff) VAD Wind Profile for 1321 UTC 12 May 1996

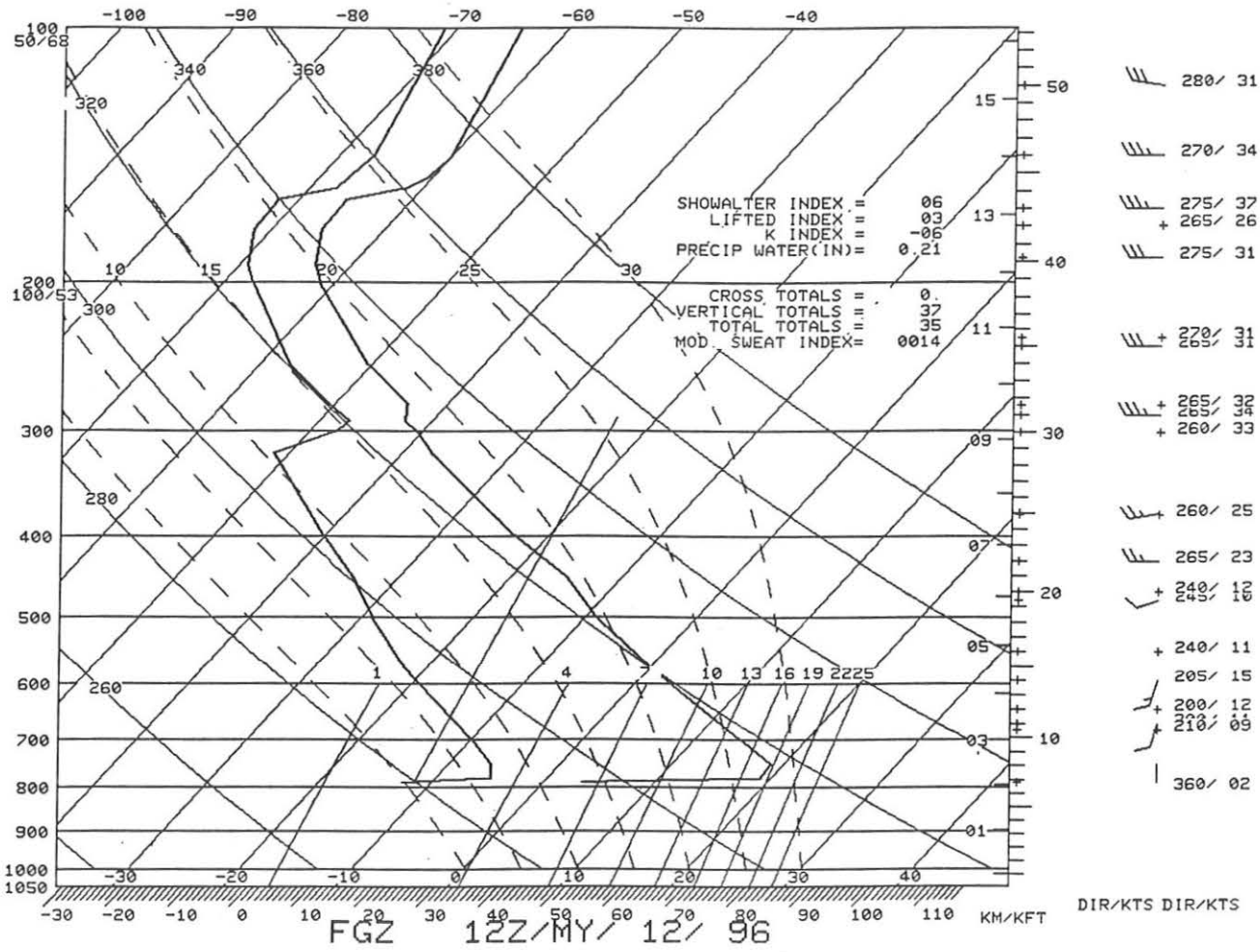

Fig. 12b FGZ (Flagstaff) sounding for 1200 UTC 12 May 1996

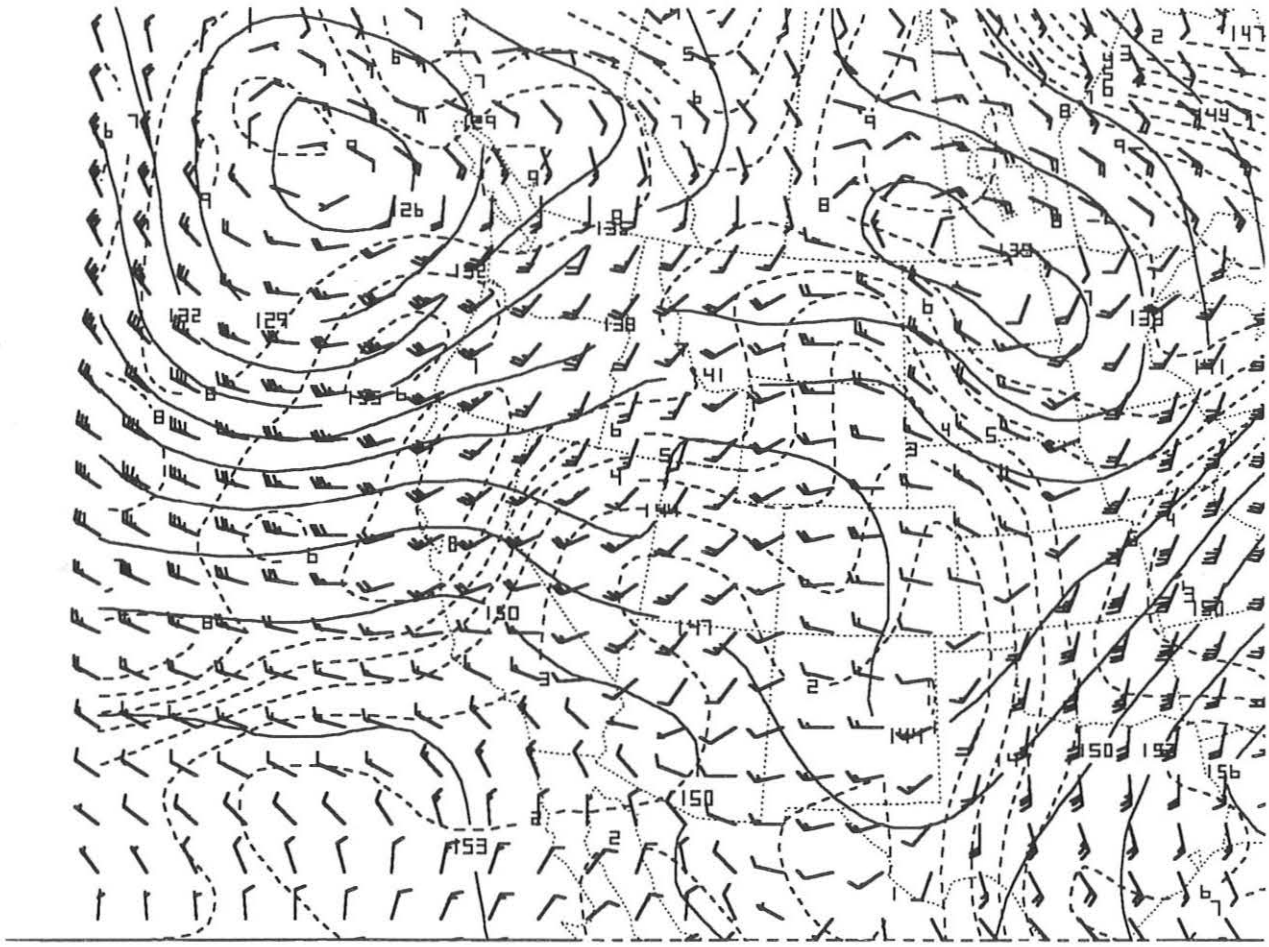

Fig. 13 ETA model PCGRIDDS initial analysis of geopotential height (dam), relative humidity (tens of %), and wind (kts) at the 850 mb level for 0000 UTC 18 May 1996

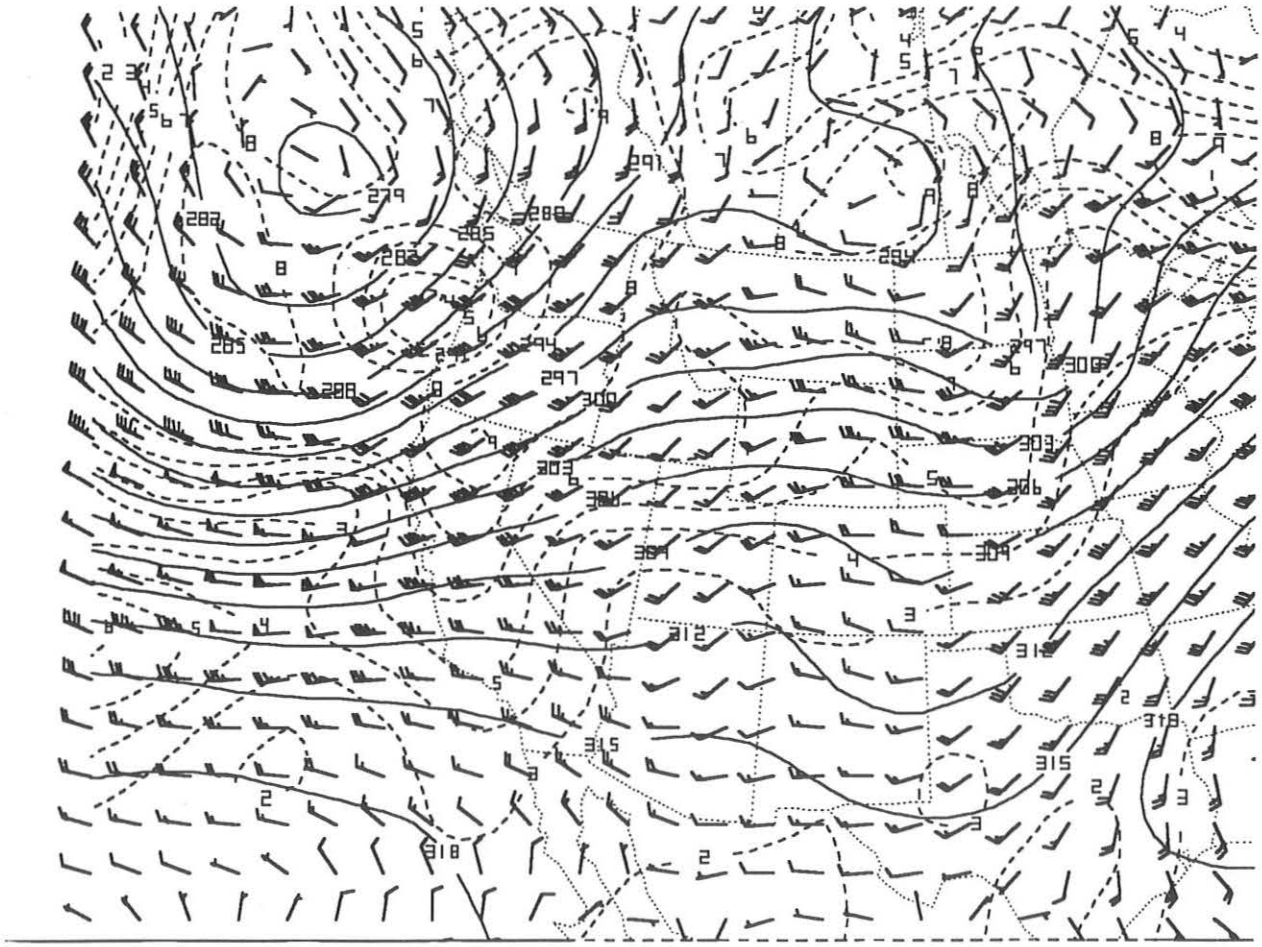

Fig. 14 ETA model PCGRIDDS initial analysis of geopotential height (dam), relative humidity (tens of %), and wind (kts) at the 700 mb level for 0000 UTC 18 May 1996

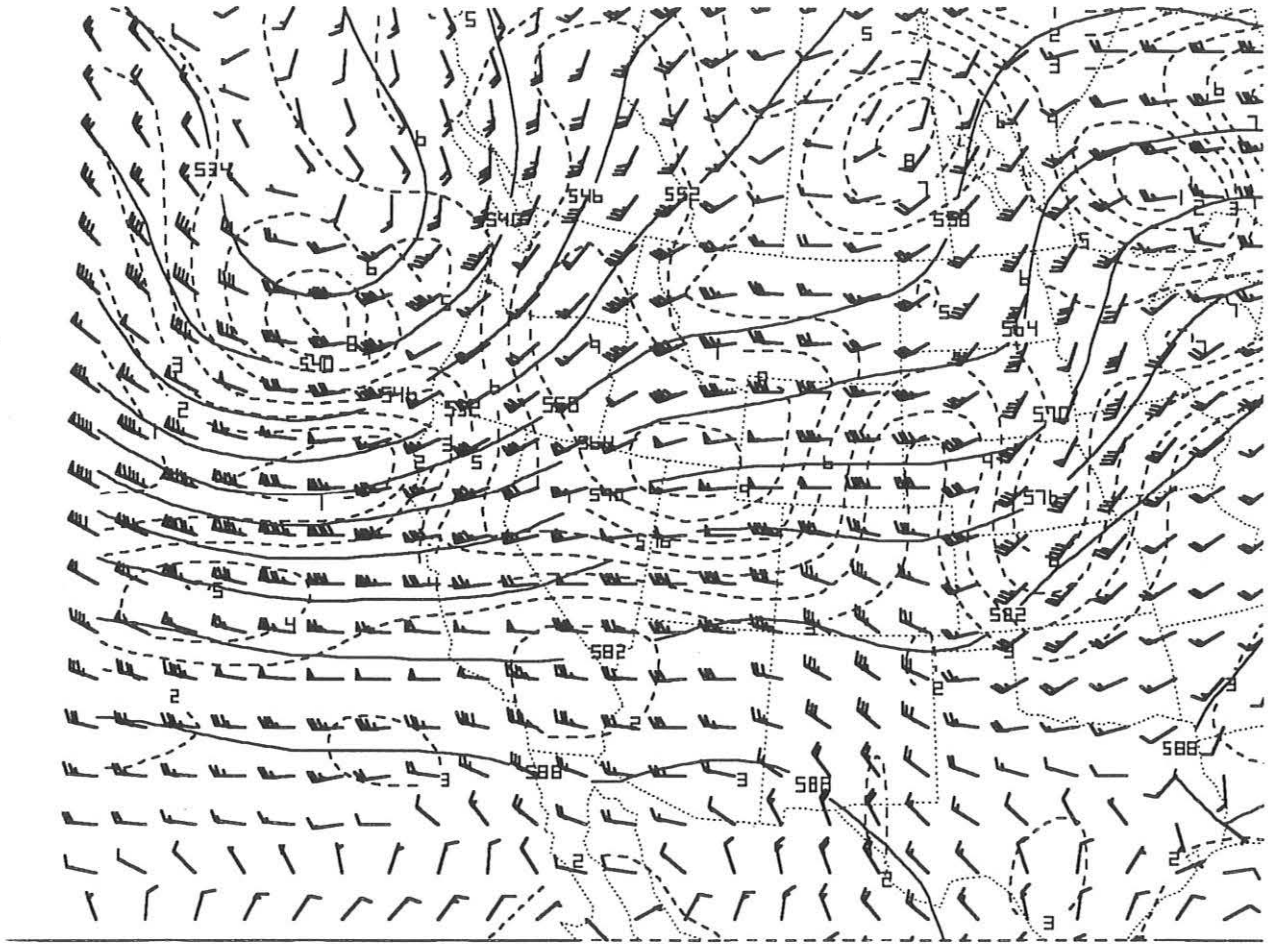

Fig. 15 ETA model PCGRIDDS initial analysis of geopotential height (dam), relative humidity (tens of %), and wind (kts) at the 500 mb level for 0000 UTC 18 May 1996

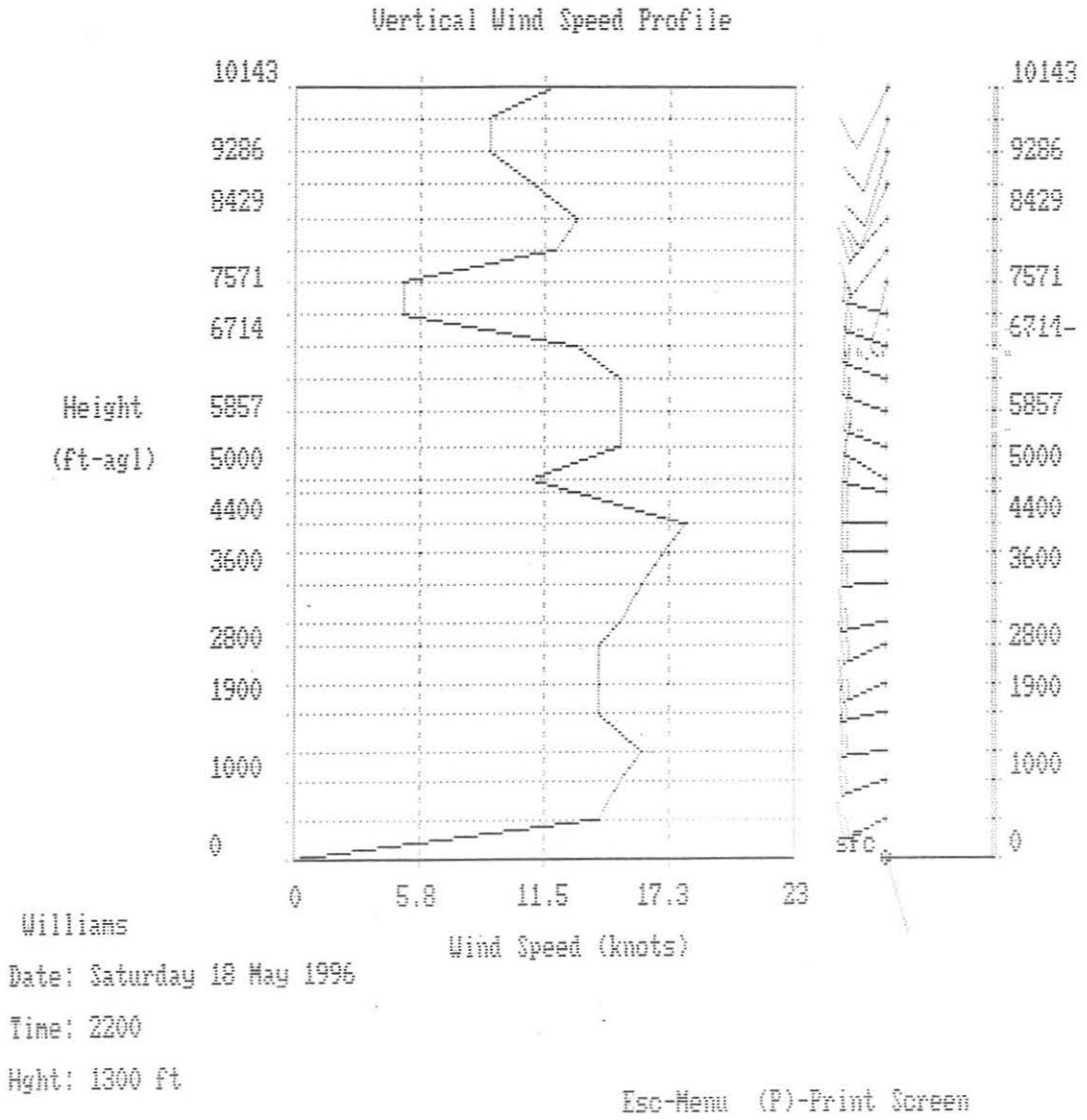

Fig. 16 Pibal flight wind speeds and direction for the period 0535-0605 UTC 18 May 1996. Flight was performed approximately 1 SM west of the KIWA radar site.

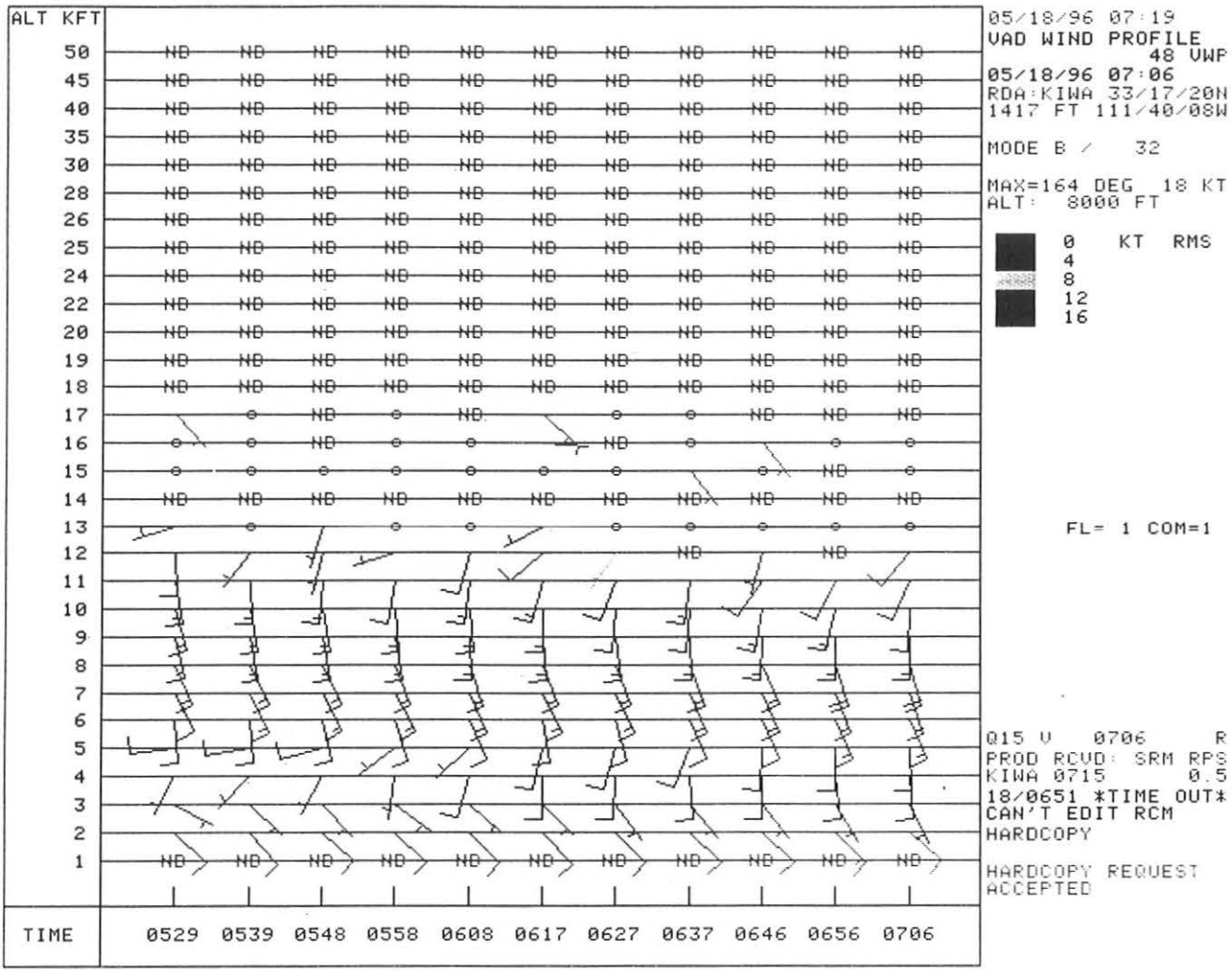

Fig. 17 KIWA (Phoenix) VAD Wind Profile for 0706 UTC 18 May 1996

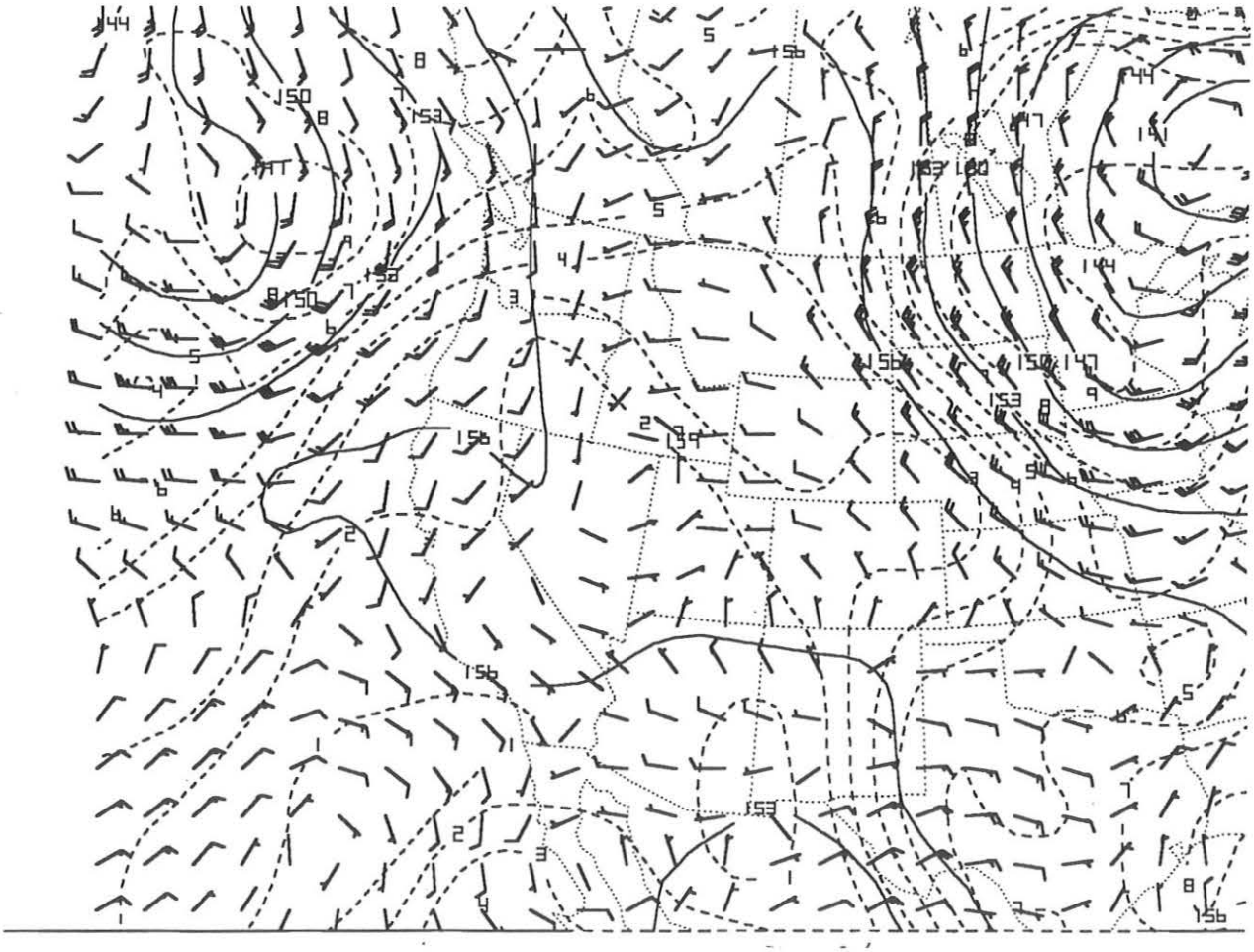

Fig. 18 ETA model PCGRIDDS initial analysis of geopotential height (dam), relative humidity (tens of %), and wind (kts) at the 850 mb level for 0000 UTC 02 June 1996

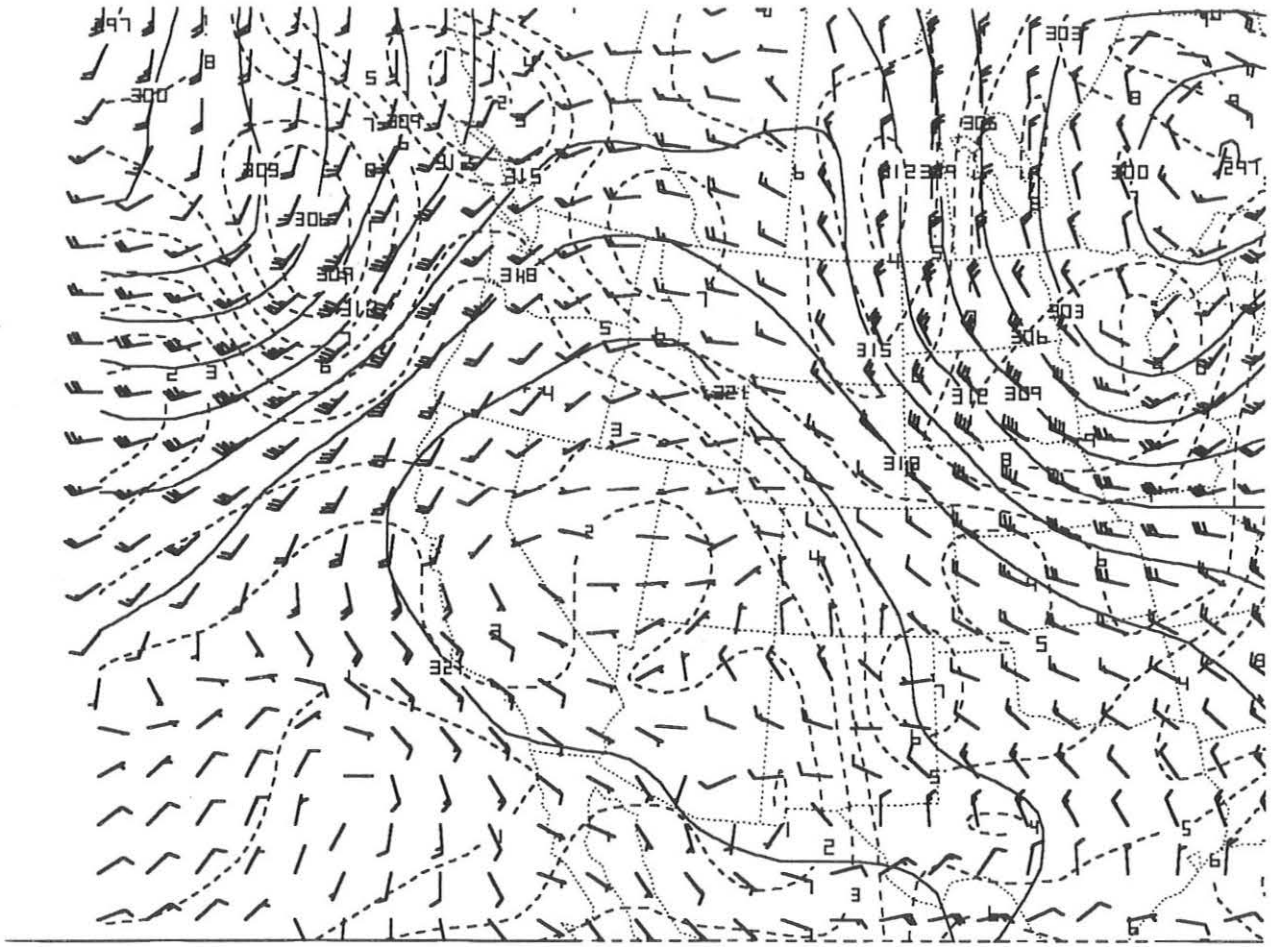

Fig. 19 ETA model PCGRIDDS initial analysis of geopotential height (dam), relative humidity (tens of %), and wind (kts) at the 700 mb level for 0000 UTC 02 June 1996

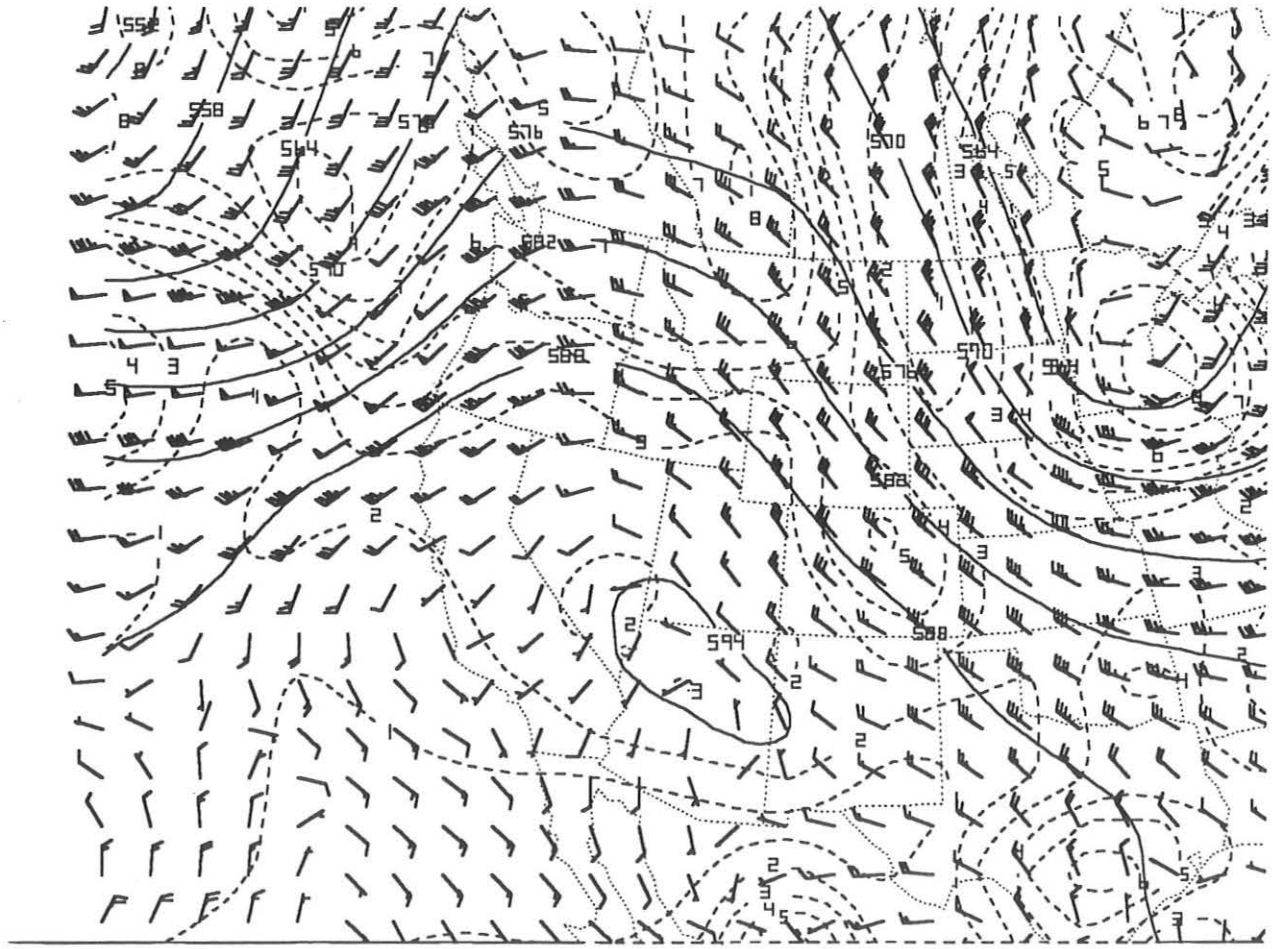

Fig. 20 ETA model PCGRIDDS initial analysis of geopotential height (dam), relative humidity (tens of %), and wind (kts) at the 500 mb level for 0000 UTC 02 June 1996

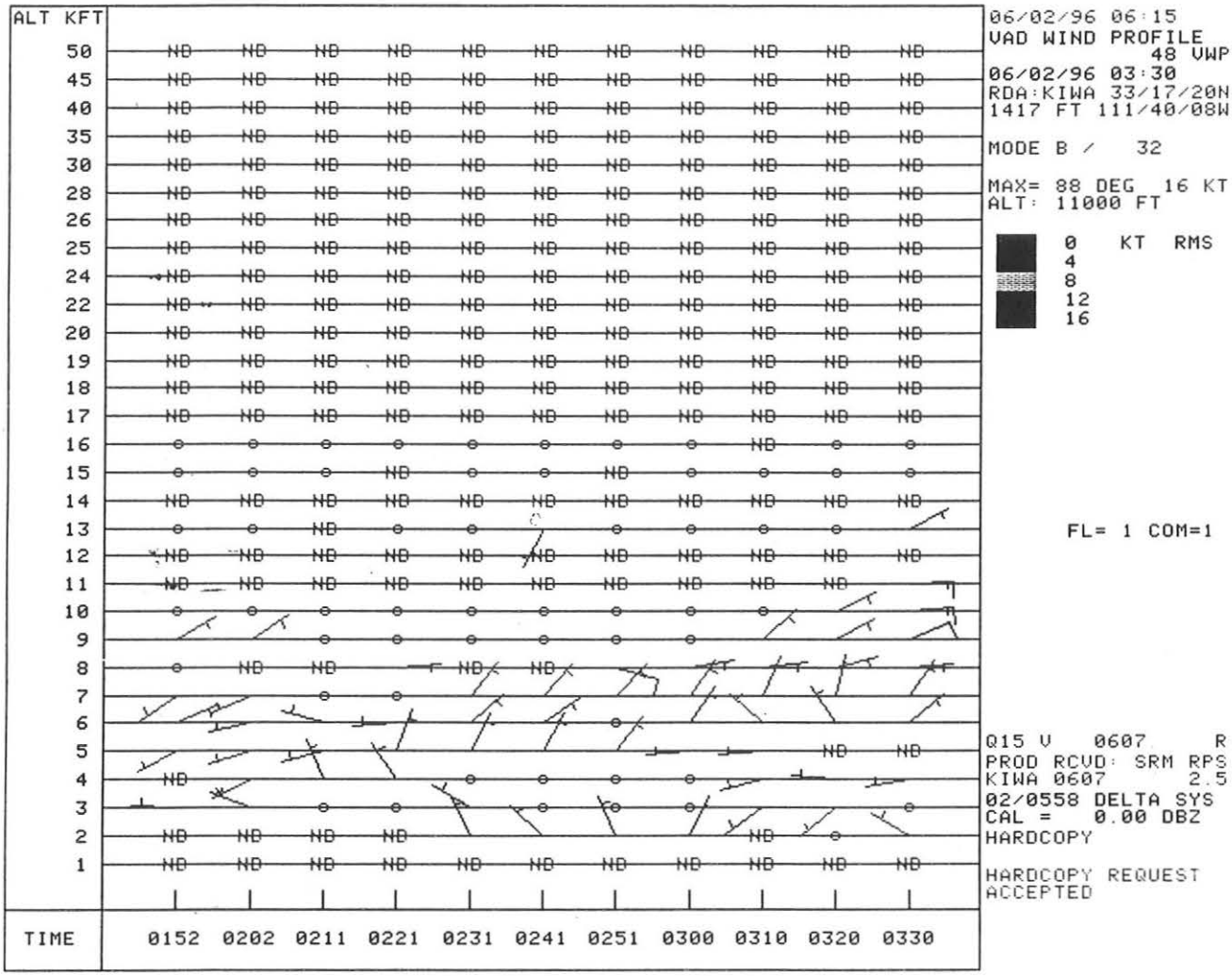

Fig. 21 KIWA (Phoenix) VAD Wind Profile for 0330 UTC 02 June 1996

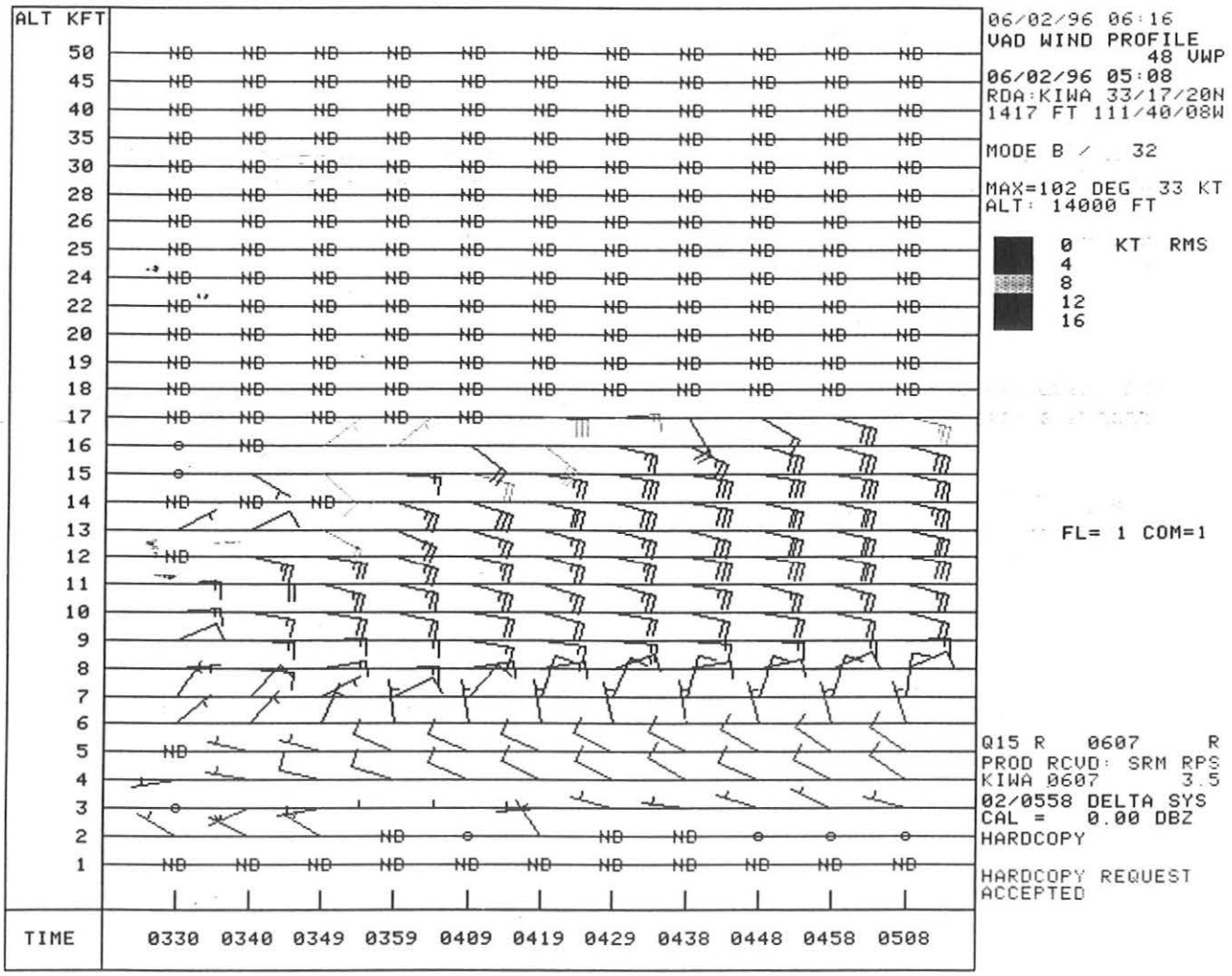

Fig. 22 KIWA (Phoenix) VAD Wind Profile for 0508 UTC 02 June 1996

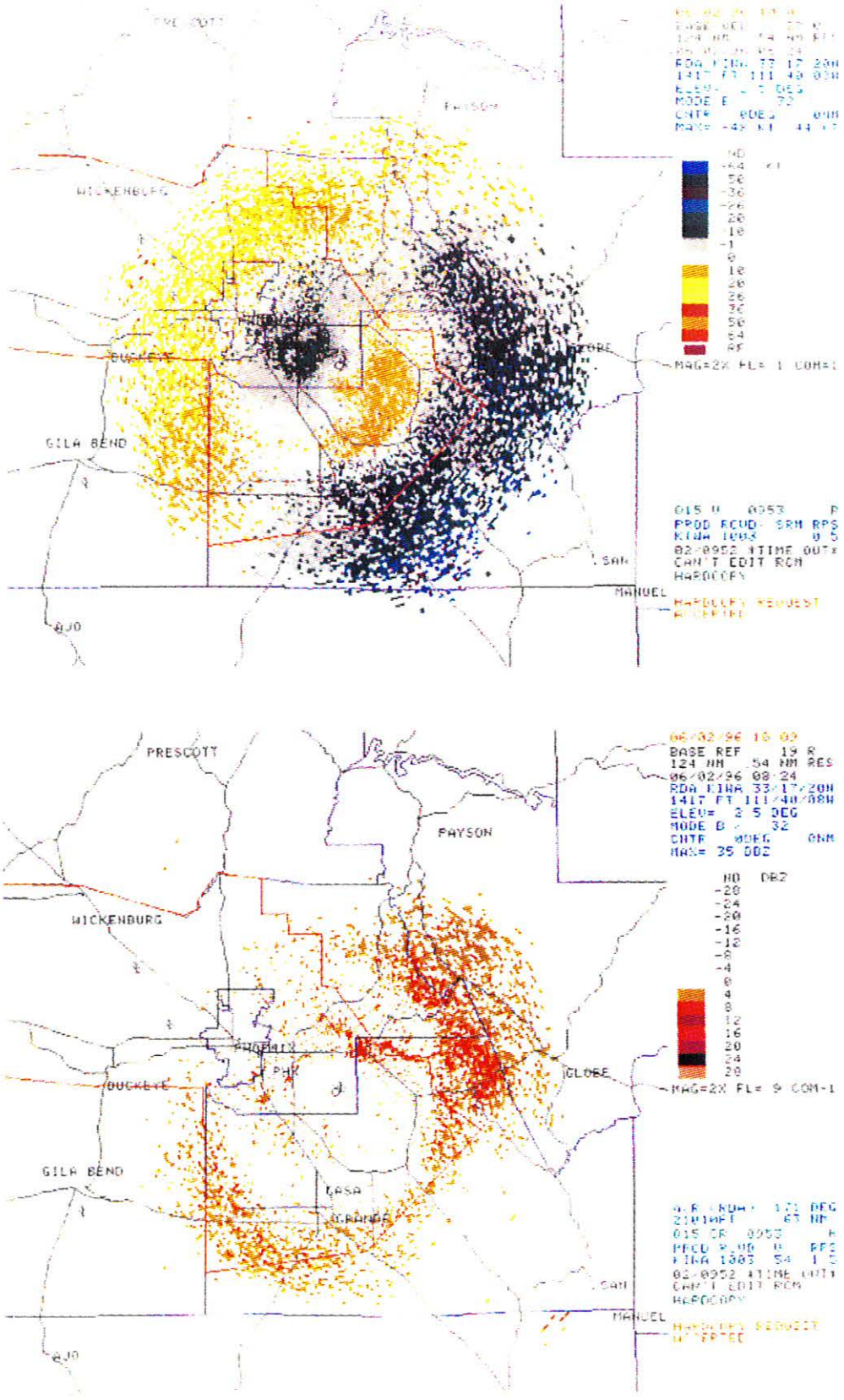

Fig. 23 (a) KIWA 2.5° Base Reflectivity and (b) Velocity products valid at 0824 UTC 02 June 1996

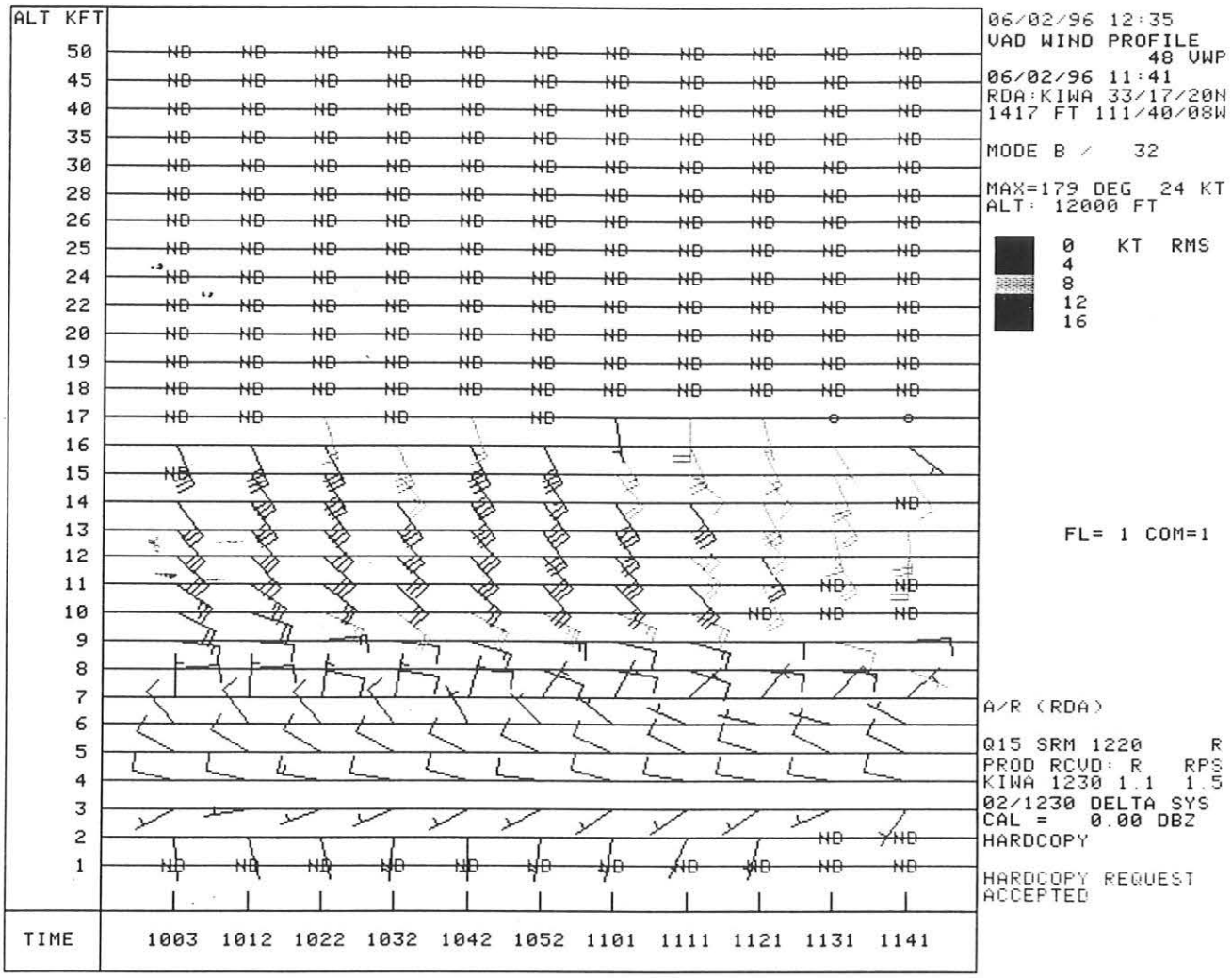

Fig. 24 KIWA (Phoenix) VAD Wind Profile for 1141 UTC 02 June 1996

144 Arizona Cool Season Climatological Surface Wind and Pressure Gradient Study. Ira S. Brenner, May 1979. (PB298900/AS)
146 The BART Experiment. Morris S. Webb, October 1979. (PB80 155112)
147 Occurrence and Distribution of Flash Floods in the Western Region. Thomas L. Dietrich, December 1979. (PB80 160344)
149 Misinterpretations of Precipitation Probability Forecasts. Allan H. Murphy, Sarah Lichtenstein, Baruch Fischhoff, and Robert L. Winkler, February 1980. (PB80 174576)
150 Annual Data and Verification Tabulation - Eastern and Central North Pacific Tropical Storms and Hurricanes 1979. Emil B. Gunther and Staff, EPHC, April 1980. (PB80 220486)
NMC Model Performance in the Northeast Pacific. James E. Overland, PMEL-ERL, April 1980. (PB80 196033)
Climate of Salt Lake City, Utah. William J. Alder, Sean T. Buchanan, William Cope (Retired), James A. Cisco, Craig C. Schmidt, Alexander R. Smith (Retired), Wilbur E. Figgins (Retired), April 1996 - Sixth Revision (PB96 175583)
153 An Automatic Lightning Detection System in Northern California. James E. Rea and Chris E. Fontana, June 1980. (PB80 225592)
154 Regression Equation for the Peak Wind Gust 6 to 12 Hours in Advance at Great Falls During Strong Downslope Wind Storms. Michael J. Oard, July 1980. (PB91 108367)
155 A Raininess Index for the Arizona Monsoon. John H. Ten Harkel, July 1980. (PB81 106494)
156 The Effects of Terrain Distribution on Summer Thunderstorm Activity at Reno, Nevada. Christopher Dean Hill, July 1980. (PB81 102501)
157 An Operational Evaluation of the Scofield/Oliver Technique for Estimating Precipitation Rates from Satellite Imagery. Richard Ochoa, August 1980. (PB81 108227)
158 Hydrology Practicum. Thomas Dietrich, September 1980. (PB81 134033)
159 Tropical Cyclone Effects on California. Arnold Court, October 1980. (PB81 133779)
160 Eastern North Pacific Tropical Cyclone Occurrences During Intraseasonal Periods. Preston W. Leftwich and Gail M. Brown, February 1981. (PB81 205494)
161 Solar Radiation as a Sole Source of Energy for Photovoltaics in Las Vegas, Nevada, for July and December. Darryl Randerson, April 1981. (PB81 224503)
162 A Systems Approach to Real-Time Runoff Analysis with a Deterministic Rainfall-Runoff Model. Robert J.C. Burnash and R. Larry Ferral, April 1981. (PB81 224495)
163 A Comparison of Two Methods for Forecasting Thunderstorms at Luke Air Force Base, Arizona. LTC Keith R. Cooley, April 1981. (PB81 225393)
164 An Objective Aid for Forecasting Afternoon Relative Humidity Along the Washington Cascade East Slopes. Robert S. Robinson, April 1981. (PB81 23078)
165 Annual Data and Verification Tabulation, Eastern North Pacific Tropical Storms and Hurricanes 1980. Emil B. Gunther and Staff, May 1981. (PB82 230336)
166 Preliminary Estimates of Wind Power Potential at the Nevada Test Site. Howard G. Booth, June 1981. (PB82 127036)
167 ARAP User's Guide. Mark Mathewson, July 1981, Revised September 1981. (PB82 196783)
168 Forecasting the Onset of Coastal Gales Off Washington-Oregon. John R. Zimmerman and William D. Burton, August 1981. (PB82 127051)
169 A Statistical-Dynamical Model for Prediction of Tropical Cyclone Motion in the Eastern North Pacific Ocean. Preston W. Leftwich, Jr., October 1981. (PB82195298)
170 An Enhanced Plotter for Surface Airways Observations. Andrew J. Spry and Jeffrey L. Anderson, October 1981. (PB82 153883)
171 Verification of 72-Hour 500-MB Map-Type Predictions. R.F. Quiring, November 1981. (PB82-158098)
172 Forecasting Heavy Snow at Wenatchee, Washington. James W. Holcomb, December 1981. (PB82-177783)
173 Central San Joaquin Valley Type Maps. Thomas R. Crossan, December 1981. (PB82 196064)
174 ARAP Test Results. Mark A. Mathewson, December 1981. (PB82 198103)
Approximations to the Peak Surface Wind Gusts from Desert Thunderstorms. Darryl Randerson, June 1982. (PB82 253089)
Climate of Phoenix, Arizona. Robert J. Schmidli and Austin Jamison, April 1969 (Revised July 1996). (PB96-191614)
178 Annual Data and Verification Tabulation, Eastern North Pacific Tropical Storms and Hurricanes 1982. E.B. Gunther, June 1983. (PB85 106078)
179 Stratified Maximum Temperature Relationships Between Sixteen Zone Stations in Arizona and Respective Key Stations. Ira S. Brenner, June 1983. (PB83 249904)
180 Standard Hydrologic Exchange Format (SHEF) Version I. Phillip A. Pasteris, Vernon C. Bissel, David G. Bennett, August 1983. (PB85 106052)
181 Quantitative and Spacial Distribution of Winter Precipitation along Utah's Wasatch Front. Lawrence B. Dunn, August 1983. (PB85 106912)
182 500 Millibar Sign Frequency Teleconnection Charts - Winter. Lawrence B. Dunn, December 1983. (PB85 106276)
183 500 Millibar Sign Frequency Teleconnection Charts - Spring. Lawrence B. Dunn, January 1984. (PB85 111367)
184 Collection and Use of Lightning Strike Data in the Western U.S. During Summer 1983. Glenn Rasch and Mark Mathewson, February 1984. (PB85 110534)
185 500 Millibar Sign Frequency Teleconnection Charts - Summer. Lawrence B. Dunn, March 1984. (PB85 111359)
186 Annual Data and Verification Tabulation eastern North Pacific Tropical Storms and Hurricanes 1983. E.B. Gunther, March 1984. (PB85 109635)
187 500 Millibar Sign Frequency Teleconnection Charts - Fall. Lawrence B. Dunn, May 1984. (PB85-110930)
188 The Use and Interpretation of Isentropic Analyses. Jeffrey L. Anderson, October 1984. (PB85-132694)
189 Annual Data & Verification Tabulation Eastern North Pacific Tropical Storms and Hurricanes 1984. E.B. Gunther and R.L. Cross, April 1985. (PB85 1878887AS)
190 Great Salt Lake Effect Snowfall: Some Notes and An Example. David M. Carpenter, October 1985. (PB86 119153/AS)
191 Large Scale Patterns Associated with Major Freeze Episodes in the Agricultural Southwest. Ronald S. Hamilton and Glenn R. Lussky, December 1985. (PB86 144474AS)
192 NWR Voice Synthesis Project: Phase I. Glen W. Sampson, January 1986. (PB86 145604/AS)
193 The MCC - An Overview and Case Study on Its Impact in the Western United States. Glenn R. Lussky, March 1986. (PB86 170651/AS)
194 Annual Data and Verification Tabulation Eastern North Pacific Tropical Storms and Hurricanes 1985. E.B. Gunther and R.L. Cross, March 1986. (PB86 170941/AS)
195 Radid Interpretation Guidelines. Roger G. Pappas, March 1986. (PB86 177680/AS)
196 A Mesoscale Convective Complex Type Storm over the Desert Southwest. Darryl Randerson, April 1986. (PB86 190998/AS)
197 The Effects of Eastern North Pacific Tropical Cyclones on the Southwestern United States. Walter Smith, August 1986. (PB87 106258AS)
198 Preliminary Lightning Climatology Studies for Idaho. Christopher D. Hill, Carl J. Gorski, and Michael C. Conger, April 1987. (PB87 180196/AS)
Heavy Rains and Flooding in Montana: A Case for Slantwise Convection. Glenn R. Lussky, April 1987. (PB87 185229/AS)
Annual Data and Verification Tabulation Eastern North Pacific Tropical Storms and Hurricanes 1986. Roger L. Cross and Kenneth B. Mielke, September 1987. (PB88 110895/AS)
201 An Inexpensive Solution for the Mass Distribution of Satellite Images. Glen W. Sampson and George Clark, September 1987. (PB88 114038/AS)
202 Annual Data and Verification Tabulation Eastern North Pacific Tropical Storms and Hurricanes 1987. Roger L. Cross and Kenneth B. Mielke, September 1988. (PB88-101935/AS)
203 An Investigation of the 24 September 1986 "Cold Sector" Tornado Outbreak in Northern California. John P. Monteverdi and Scott A. Braun, October 1988. (PB89 121297/AS)
204 Preliminary Analysis of Cloud-To-Ground Lightning in the Vicinity of the Nevada Test Site. Carven Scott, November 1988. (PB89 128649/AS)
205 Forecast Guidelines For Fire Weather and Forecasters -- How Nighttime Humidity Affects Wildland Fuels. David W. Goens, February 1989. (PB89 162549/AS)
206 A Collection of Papers Related to Heavy Precipitation Forecasting. Western Region Headquarters, Scientific Services Division, August 1989. (PB89 230833/AS)
207 The Las Vegas McCarran International Airport Microburst of August 8, 1989. Carven A. Scott, June 1990. (PB90-240268)
208 Meteorological Factors Contributing to the Canyon Creek Fire Blowup, September 6 and 7, 1988. David W. Goens, June 1990. (PB90-245085)
209 Stratus Surge Prediction Along the Central California Coast. Peter Felsch and Woodrow Whitlatch, December 1990. (PB91-129239)
210 Hydrotools. Tom Egger. January 1991. (PB91-151787/AS)
211 A Northern Utah Soaker. Mark E. Struthwolf, February 1991. (PB91-168716)
212 Preliminary Analysis of the San Francisco Rainfall Record: 1849-1990. Jan Null, May 1991. (PB91-208439)
213 Idaho Zone Preformat, Temperature Guidance, and Verification. Mark A. Mollner, July 1991. (PB91-227405/AS)
214 Emergency Operational Meteorological Considerations During an Accidental Release of Hazardous Chemicals. Peter Mueller and Jerry Galt, August 1991. (PB91-235424)
215 WeatherTools. Tom Egger, October 1991. (PB93-184950)
216 Creating MOS Equations for RAWS Stations Using Digital Model Data. Dennis D. Gettman, December 1991. (PB92-131473/AS)
217 Forecasting Heavy Snow Events in Missoula, Montana. Mike Richmond, May 1992. (PB92-196104)
218 NWS Winter Weather Workshop in Portland, Oregon. Various Authors, December 1992. (PB93-146785)
219 A Case Study of the Operational Usefulness of the Sharp Workstation in Forecasting a Mesocyclone-Induced Cold Sector Tornado Event in California. John P. Monteverdi, March 1993. (PB93-178697)
220 Climate of Pendleton, Oregon. Claudia Bell, August 1993. (PB93-227536)
221 Utilization of the Bulk Richardson Number, Helicity and Sounding Modification in the Assessment of the Severe Convective Storms of 3 August 1992. Eric C. Evenson, September 1993. (PB94-131943)
222 Convective and Rotational Parameters Associated with Three Tornado Episodes in Northern and Central California. John P. Monteverdi and John Quadros, September 1993. (PB94-131943)
223 Climate of San Luis Obispo, California. Gary Ryan, February 1994. (PB94-162062)
224 Climate of Wenatchee, Washington. Michael W. McFarland, Roger G. Buckman, and Gregory E. Matzen, March 1994. (PB94-164308)
225 Climate of Santa Barbara, California. Gary Ryan, December 1994. (PB95-173720)
226 Climate of Yakima, Washington. Greg DeVoir, David Hogan, and Jay Neher, December 1994. (PB95-173688)
227 Climate of Kalispell, Montana. Chris Maier, December 1994. (PB95-169488)
228 Forecasting Minimum Temperatures in the Santa Maria Agricultural District. Wilfred Pi and Peter Felsch, December 1994. (PB95-171088)
229 The 10 February 1994 Oroville Tornado--A Case Study. Mike Staudenmaier, Jr., April 1995. (PB95-241873)
230 Santa Ana Winds and the Fire Outbreak of Fall 1993. Ivory Small, June 1995. (PB95-241865)
231 Washington State Tornadoes. Tresté Huse, July 1995. (PB96-107024)
232 Fog Climatology at Spokane, Washington. Paul Frisbie, July 1995. (PB96-106604)
233 Storm Relative Isentropic Motion Associated with Cold Fronts in Northern Utah. Kevin B. Baker, Kathleen A. Hadley, and Lawrence B. Dunn, July 1995. (PB96-106596)
234 Some Climatological and Synoptic Aspects of Severe Weather Development in the Northwestern United States. Eric C. Evenson and Robert H. Johns, October 1995. (PB96-112958)
235 Climate of Las Vegas, Nevada. Paul H. Skrbac and Scott Cordero, December 1995. (PB96-135553)
236 Climate of Astoria, Oregon. Mark A. McInerney, January 1996.
237 The 6 July 1995 Severe Weather Events in the Northwestern United States: Recent Examples of SSWEs. Eric C. Evenson, April 1996.
238 Significant Weather Patterns Affecting West Central Montana. Joe Lester, May 1996. (PB96-178751)
239 Climate of Portland, Oregon. Clinton C. D. Rocky, May 1996. (PB96-17603)
240 Downslop Winds of Santa Barbara, CA. Gary Ryan, July 1996 (PB96-191697)
241 Operational Applications of the Real-time National Lightning Detection Network Data at the NWSO Tucson, AZ. Darren McCollum, David Bright, Jim Meyer, and John Glueck, September 1996. (PB97-108450)
242 Climate of Pocatello, Idaho. Joe Heim, October 1996. (PB97-114540)
243 Climate of Great Falls. Montana. Matt Jackson and D. C. Williamson, December 1996.

NOAA SCIENTIFIC AND TECHNICAL PUBLICATIONS

The National Oceanic and Atmospheric Administration was established as part of the Department of Commerce on October 3, 1970. The mission responsibilities of NOAA are to assess the socioeconomic impact of natural and technological changes in the environment and to monitor and predict the state of the solid Earth, the oceans and their living resources, the atmosphere, and the space environment of the Earth.

The major components of NOAA regularly produce various types of scientific and technical information in the following kinds of publications.

PROFESSIONAL PAPERS–Important definitive research results, major techniques, and special investigations.

CONTRACT AND GRANT REPORTS–Reports prepared by contractors or grantees under NOAA sponsorship.

ATLAS–Presentation of analyzed data generally in the form of maps showing distribution of rainfall, chemical and physical conditions of oceans and atmosphere, distribution of fishes and marine mammals, ionospheric conditions, etc.

TECHNICAL SERVICE PUBLICATIONS – Reports containing data, observations, instructions, etc. A partial listing includes data serials; prediction and outlook periodicals; technical manuals, training papers, planning reports, and information serials; and miscellaneous technical publications.

TECHNICAL REPORTS–Journal quality with extensive details, mathematical developments, or data listings.

TECHNICAL MEMORANDUMS–Reports of preliminary, partial, or negative research or technology results, interim instructions, and the like.

Information on availability of NOAA publications can be obtained from:

NATIONAL TECHNICAL INFORMATION SERVICE

U. S. DEPARTMENT OF COMMERCE

5285 PORT ROYAL ROAD

SPRINGFIELD, VA 22161